https://doi.org/10.5194/egusphere-2025-251
Preprint. Discussion started: 24 February 2025

Influence of oceanic ventilation and terrestrial transport on the atmospheric volatile chlorinated hydrocarbons over the Western Pacific

Shan-Shan Liu [a, b, 1], Jie Ni [a, 1], Jin- Ming Song [b], Xu-Xu Gao [a], Zhen He [a, c, *], Gui-Peng Yang [a, c, d, **]

[a] Frontiers Science Center for Deep Ocean Multispheres and Earth System, and Key Laboratory of Marine Chemistry Theory and Technology, Ministry of Education, Ocean University of China, Qingdao 266100, China

[b] Key Laboratory of Marine Ecology and Environmental Sciences, Institute of Oceanology, Chinese Academy of Sciences, Qingdao 266071, China

[c] Laboratory for Marine Ecology and Environmental Science, Qingdao Marine Science and Technology Center, Qingdao 266237, China

[d] Institute of Marine Chemistry, Ocean University of China, Qingdao 266100, China

Abstract

Volatile chlorinated hydrocarbons (VCHCs), key ozone-depleting substances and greenhouse gases, depend on oceanic emission and uptake for their atmospheric budget. However, data on VCHCs in the Western Pacific remain limited. This study investigated the distribution and sources of VCHCs ($CHCl_3$, C_2HCl_3, CCl_4, and CH_3CCl_3) in the Western Pacific during 2019-2020. Elevated seawater concentrations of $CHCl_3$ and C_2HCl_3 in the Kuroshio-Oyashio Extension (KOE) were driven by mesoscale eddies enhancing primary productivity, while CCl_4 and CH_3CCl_3 concentrations were mainly influenced by atmospheric inputs. Atmospheric

[1] Shan-Shan Liu and Jie Ni contributed equally to the paper.

[*] Corresponding author. Key Laboratory of Marine Chemistry Theory and Technology, Ministry of Education, Ocean University of China, Qingdao 266100, China

[**] Corresponding author. Institute of Marine Chemistry, Ocean University of China, Qingdao 266100, China

E-mail addresses: zhenhe@ouc.edu.cn (Z. He), gpyang@mail.ouc.edu.cn (G.-P. Yang)

https://doi.org/10.5194/egusphere-2025-251
Preprint. Discussion started: 24 February 2025

concentrations of VCHCs decreased from coastal to open ocean areas, with terrestrial air masses from Eastern Asia contributing significantly. Additionally, atmospheric $CHCl_3$ and C_2HCl_3 concentrations were positively correlated with Chl-*a* in the KOE region. These findings suggested that both atmospheric transport from the continent and ocean emissions could influence $CHCl_3$ and C_2HCl_3 levels. However, analysis of sea-to-air fluxes and saturation anomalies showed that atmospheric transport primarily influenced atmospheric $CHCl_3$ and C_2HCl_3 concentrations. The estimated sea-to-air flux indicated that the Western Pacific acted as a source for $CHCl_3$ and C_2HCl_3 but a sink for CCl_4 and CH_3CCl_3, with the potential to absorb 17 ± 2% of CCl_4 emissions from Eastern China, 7 ± 5% from Eastern Asia, and 3 ± 1% of global emissions. Additionally, this region accounted for 8 ± 4% of the global oceanic absorption of CCl_4. These findings underscored the Western Pacific's key role in regulating atmospheric CCl_4 concentrations and mitigating its accumulation in Eastern Asia, providing essential data for global VCHCs emission and uptake estimates.

https://doi.org/10.5194/egusphere-2025-251
Preprint. Discussion started: 24 February 2025

Graphical abstract

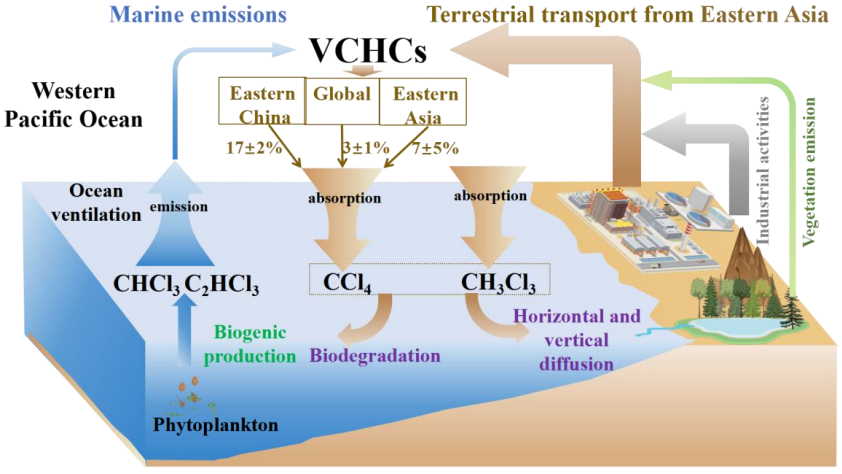

Introduction

Volatile halocarbons (VHCs) are ozone-depleting substances and greenhouse gases (Abrahamsson et al., 1995; Abrahamsson and Edkahl, 1996). As an important component of VHCs, volatile chlorinated hydrocarbons (VCHCs) are believed to be important carriers of chlorine to the stratosphere. Among them, carbon tetrachloride (CCl_4), chloroform ($CHCl_3$), methyl chloroform (CH_3CCl_3), and trichloroethene (C_2HCl_3) account for an estimated 11% of the total organic chlorine in the troposphere (WMO, 2022). CCl_4 and CH_3CCl_3 are categorized as long-lived halocarbons, having atmospheric lifetimes exceeding six months. They are evenly distributed throughout the troposphere except where there are local sources. They are major contributors to both the greenhouse effect and ozone depletion, and their usage and emissions are subject to regulation under the Montreal Protocol (1987). In contrast, C_2HCl_3 and $CHCl_3$ are considered very short-lived halocarbons (VSLSs) (typically less than six months) and are currently unregulated by the Montreal Protocol. Nevertheless, a significant portion of VSLSs and their degradation products reach the stratosphere, with over 80% of chlorinated VSLSs estimated to reach these altitudes (Carpenter et

https://doi.org/10.5194/egusphere-2025-251
Preprint. Discussion started: 24 February 2025

al., 2014). VSLSs have been shown to have disproportionately large impacts on radiative forcing and climate as they break down in the atmosphere and subsequently deplete the ozone, this is especially impactful because they occur at lower altitudes more sensitive to climate changes (Hossaini et al., 2015; Hossaini et al., 2017; An et al., 2023; Saiz-Lopez et al., 2023).

The oceans, acting as source and sink of VCHCs (C_2HCl_3, $CHCl_3$, CCl_4, and CH_3CCl_3), play a significant role in the biogeochemical cycling of VCHCs (Blake et al., 2003; Karlsson et al., 2008; Butler et al., 2016). $CHCl_3$ and C_2HCl_3 in the oceans come from both anthropogenic and natural sources (Abrahamsson and Edkahl, 1996; Moore, 2003; Karlsson et al., 2008; He et al., 2013c). Previous studies have revealed that marine microalgae (Scarratt et al., 1999; Lim et al., 2018), macroalgae (Gschwend et al., 1985; Abrahamsson et al., 1995), and various other marine organisms (Khan et al., 2011) act as natural sources of $CHCl_3$ and C_2HCl_3. The tropical diatoms, the cyanobacterium *Synechococcus* and the chlorophyte *Parachlorella*, and purple sulfur bacteria, have been shown to produce $CHCl_3$ (Scarratt et al., 1999; Plummer et al., 2002; Lim et al., 2018). Moreover, $CHCl_3$ emissions have also been found in regions like the Antarctic tundra (Zhang et al., 2021), Dead Sea landscapes (Schechner et al., 2019), and coastal wetlands affected by sea level rise (Jiao et al., 2018), entering the ocean via land runoff and atmospheric deposition. Abrahamsson et al. (1995) argued that C_2HCl_3 emissions from algae to the atmosphere are present in non-negligible amounts within the global atmospheric chlorine budget. Anthropogenic emissions of $CHCl_3$ mainly come from their use as a raw material in refrigerant hydrochlorofluorocarbon-22 (HCFC-22) production (> 95%) and as a by-product of the water chlorination and bleaching processes in the pulp and paper industry (McCulloch, 2003). C_2HCl_3 is also emitted from its use as a

https://doi.org/10.5194/egusphere-2025-251
Preprint. Discussion started: 24 February 2025

solvent and as feedstock in producing HFCs and other chemicals (Chipperfield et al., 2020). Notably, while the Montreal Protocol regulates the use of HCFC-22 in dispersive applications, demand for the refrigerant as a feedstock in the manufacture of fluoropolymers production is surging (Say et al., 2020). Anthropogenic emissions of $CHCl_3$ and C_2HCl_3 ultimately enter the ocean through land runoff and atmospheric deposition, especially in coastal and estuarine regions (Yokouchi et al., 2005). The sources of CH_3CCl_3 and CCl_4 in the oceans are largely anthropogenic (Butler et al., 2016; WMO, 2022). As a primary component of cleaning agents, dry-cleaning solvents, and degreasing agents, CH_3CCl_3 previously saw widespread use (Wang et al., 1995). CCl_4 was previously extensively used in chlorine gas production, industrial bleaching, organic chemical solvents, and fire extinguisher production (Rigby et al., 2014). Moreover, these two gases are used as solvents and feedstock chemicals in producing HFCs and other chemicals (Chipperfield et al., 2020). Although their usage is banned in the Montreal Protocol (1987) and its amendments and adjustments, unregulated emissions persist from specific manufacturing activities. For example, Liang et al. (2016) and Sherry et al. (2018) showed that CCl_4 production is linked to non-feedstock emissions associated with chloromethane and perchloroethylene manufacturing facilities. They also demonstrated that up to 10 Gg yr^{-1} of CCl_4 emissions may be produced by unreported, unintentional release during chlorine production, including emissions from chlor-alkali plants and their use in industrial and domestic bleaching. Additionally, Li et al. (2024) identified potential industrial sources of CCl_4 emissions, such as the manufacture of general-purpose machinery, raw chemical materials, and chemical products.

Substantial spatial and temporal variabilities characterize the distributions of VCHCs in oceans, with higher concentrations in estuaries than nearshore zones, and

https://doi.org/10.5194/egusphere-2025-251
Preprint. Discussion started: 24 February 2025

higher concentrations in nearshore zones than the open ocean. These distributions are mainly influenced by anthropogenic emissions from terrestrial sources (Yokouchi et al., 2005; Bravo-Linares et al., 2007; Liang et al., 2014) and by the biological processes of algae in nearshore zones (Christof et al., 2002; Karlsson et al., 2008; Yang et al., 2015). In addition, the distributions of VCHCs are related to various factors, including source strength, season, topography, tides, and water masses (Yang et al., 2015; Liu et al., 2021). Previous studies have pointed out that land-based inputs have significant impacts on the distributions of marine VCHCs because VCHCs from human activities exceed marine emissions (Lunt et al., 2018; Fang et al., 2019; An et al., 2021; Yi et al., 2023). For example, persistent large emissions of CCl_4 from Eastern Asia, accounting for approximately 40% of global emissions (Lunt et al., 2018), coincided with a global increase in CCl_4 mole fractions between 2010 and 2015, as noted by Fang et al. (2019). This growth, notably driven by eastern China, has potential implications for Antarctic ozone layer recovery. However, according to the latest data from WMO (2022), the CCl_4 emissions from eastern China showed a significant decline from 2016 to 2019, dropping from 11.3 ± 1.9 Gg yr^{-1} in 2016 to 6.3 ± 1.1 Gg yr^{-1} in 2019. Similarly, An et al. (2023) reported a decline in $CHCl_3$ emissions from China, which peaked at 193 Gg yr^{-1} in 2017 and decreased to 147 Gg yr^{-1} by 2018, where, as of 2020, it has remained relatively constant. Yu et al. (2020) demonstrated a successful reduction in China CH_3CCl_3 emissions from 1.6 Gg yr^{-1} in 2007 to 0.3 Gg yr^{-1} in 2013, demonstrating compliance with the Montreal Protocol. Despite these declines in VCHCs emissions, Eastern Asia continues to be an important source of global VCHCs emissions (WMO, 2022).

The Western Pacific exerts a profound influence on sea-to-air exchanges and the global biogeochemical cycles of materials (Tsunogai, 2002; Shi et al., 2022). The

https://doi.org/10.5194/egusphere-2025-251
Preprint. Discussion started: 24 February 2025

dynamic western boundary currents, equatorial Pacific circulation systems, and the expansive Western Pacific Warm Pool play pivotal roles in vertical water mass transport and material/heat exchange between the equatorial and subtropical Pacific regions (Hu et al., 2015). These oceanic processes likely impact the variations in emissions of VCHCs in the Western Pacific. Additionally, owing to its proximity to land, encompassing regions such as the Philippines and Japan, atmospheric vertical diffusion and pollutant transport from land may significantly influence atmospheric VCHCs levels over the Western Pacific (Lunt et al., 2018). While a few studies have observed seawater and atmospheric VCHCs in the North Pacific (Quack and Suess, 1999; Liu et al., 2021), comprehensive data on atmospheric and seawater VCHCs in the Western Pacific remain scarce. Consequently, substantial uncertainties persist in estimates of oceanic sources and sinks of VCHCs (Blake et al., 2003; Butler et al., 2016). A noticeable research gap exists concerning our understanding of VCHCs in the Western Pacific. Furthermore, the lack of comprehensive knowledge regarding the biogeochemical factors that control VCHCs concentrations and sea-air fluxes produces uncertainties in global emission estimates.

In this study, a comprehensive field investigation was carried out in the Western Pacific with two primary objectives. Firstly, the study aimed to understand how oceanic physical and biogeochemical processes influence the distributions and emissions of these climatic VCHCs by examining various sources. Secondly, the study sought to ascertain the influence of the Western Pacific on the levels of volatile VCHCs in the atmosphere, evaluating whether it acts primarily as a source or sink of these VCHCs. Investigating the distributions of VCHCs in both the seawater and the atmosphere, along with determining their sea-air fluxes, is essential for evaluating their potential impacts on the global halogen cycle.

https://doi.org/10.5194/egusphere-2025-251
Preprint. Discussion started: 24 February 2025

2 Materials and methods

2.1 Study area

Our measurements were conducted on board the R/V "Dongfanghong 3" from October 31 to December 1, 2019, and the R/V "Science" from October 3, 2019, to January 5, 2020. Fig. 1 shows the locations of the sampling sites. The Western Pacific survey area was divided into the Kuroshio-Oyashio Extension (KOE), North Pacific Subtropical Gyre (NPSG), and Western Pacific Warm Pool (WPWP) based on oceanographic features (supplementary information, Text S1), including water temperature, salinity, and the 29 °C isotherm of surface seawater (Fig. S1, S3). These cruises covered a wide area, ranging from coastal areas to remote marine areas and from tropical areas to subtropical areas. During these cruises, we obtained data from several transects, which are presented here as two separate directions: the South-North (S-N) direction (from 2°S to 40°N) and the East-West (E-W) direction (from 130°E to 165°E). The circulation patterns of the Western Pacific, depicted in Fig. 1B, are intricate and encompass multiple oceanic currents, including the Oyashio Current (OC), the North Equatorial Current (NEC), the North Equatorial Counter Current (NECC), the Mindanao Current (MC), and the Kuroshio Current (KC). The semi-permanent Mindanao Eddy (ME) and the seasonal Halmahera Eddy (HE) are also prominent in this region. This intricate marine circulation system and the intense ocean-atmosphere interactions bestow the Northwest Pacific with a pivotal role in oceanic environmental changes, water mass exchanges, nutrient and heat transport, global biogeochemical cycles, and climatic transitions (Hu et al., 2020). Further, with the planet's largest warm pool and most robust tropical convection, the WPWP area is a critical player in global sea-air substance exchange. The meteorological patterns in this area are also significantly influenced by the Indo-Australian monsoon (Wang et

https://doi.org/10.5194/egusphere-2025-251
Preprint. Discussion started: 24 February 2025

al., 2004; Li et al., 2019a). Thus, the combined forces of the NEC-MC-KC system and the region's distinct meteorological conditions inevitably modulate the biogeochemical cycling of VCHCs in both seawater and the atmosphere.

2.2 Analysis of VCHCs in air

Atmospheric samples were collected by 3 L pre-evacuated stainless-steel Summa polished canisters (SilconCan, Restek Co., Ltd) that were pre-cleaned to measure VCHCs concentrations at ambient pressure. These sampling canisters underwent an intensive cleaning process using an automated cleaning system (Nutech 2010 DS) prior to sample collection. To avoid ship exhaust contamination, sampling was conducted upwind on the ship's top deck during low-speed transit. All atmospheric samples were analyzed within one month after the completion of the cruises. Meteorological parameters such as wind speed and direction were measured by shipboard sensors at a height of 10 m above the sea surface.

The concentrations of VCHCs in the atmosphere were assessed using a method that couples a three-stage cold trap preconcentrator (Nutech 8900DS) with a gas chromatography-mass spectrometry instrument (GC-MS, Agilent 7890A/5975C) in selective ion monitoring mode. Specifically, atmospheric samples underwent preconcentration using the three-stage cold trap preconcentrator, which removed atmospheric constituents such as H_2O and CO_2. The concentrated samples were subsequently analyzed with the GC-MS. A 10 ppbv VCHCs standard gas (Spectra Gases) was diluted using a dynamic dilution instrument (Nutech 2202A). A series of standard gas volumes were then analyzed using the same method as for the VCHCs samples to generate a standard curve for VCHCs (correlation coefficient > 0.996). All peak values of atmospheric samples were within the range of this standard curve. The analytical and calibration approach for VCHCs in the atmosphere closely mirrored

https://doi.org/10.5194/egusphere-2025-251
Preprint. Discussion started: 24 February 2025

methods utilized in previous studies (Li et al., 2019b; Yuan et al., 2019). The detection limits for the target compounds in this method ranged between 0.10 pptv and 1.0 pptv, with a relative standard deviation of 3% to 6% (Table S1).

2.3 Analysis of VCHCs in seawater

Surface seawater (0–5 m) samples were collected using a 12 L Niskin sampler equipped with a temperature-salinity-depth probe (CTD). The samples were shifted to 100 mL air-tight glass syringes without headspace. Seawater samples were preserved in a 4 °C dark environment and assayed within 12 h of collection. In addition, sea surface temperature (SST) and salinity in the study area were gauged using a CTD device.

Seawater samples were analyzed for VCHCs by coupling cold trap purge-and-trap with gas chromatography (GC-ECD, Agilent 6890A). Briefly, seawater samples (100 mL) were transferred to a purge-and-trap apparatus and purged with high-purity nitrogen at a flow rate of 60 mL min^{-1} for 14 min. The purged VCHCs were sequentially passed through glass tubes containing magnesium perchlorate ($MgClO_4$) and sodium hydroxide (NaOH) for drying and CO_2 removal, followed by enrichment onto a trap column (length: 30 cm; diameter: 0.8 mm) immersed in liquid nitrogen. The trap was subsequently heated with boiling water, and the desorbed gases were introduced into the GC using high-purity nitrogen. A DB-624 capillary column (60 m in length, 0.32 mm ID, and 1.8 μm film thickness) was employed to separate VCHCs. The initial temperature of the column was maintained at 45 °C for 10 min, then increased to 200 °C at a rate of 15 °C per minute, and held at this final temperature for 5 min. The inlet port and detector temperatures were set at 110 °C and 275 °C, respectively. The flow rate of the carrier gas, ultrapure nitrogen (N_2), was 2.1 mL min^{-1}. Identification and quantification of the VCHCs in seawater

https://doi.org/10.5194/egusphere-2025-251
Preprint. Discussion started: 24 February 2025

were based on retention times and liquid standards purchased from o2si in the US (purity > 99%). The liquid standards were diluted twice with methanol (Merck, Darmstadt, Germany, suitable for purging and analysis) to obtain the desired standard concentrations. Using the same analytical method as for the surface seawater samples, the deep seawater (5000 m) was purged with high-purity N_2 to remove the background VCHCs, and standard curves were established by diluting VCHCs standards in series (correlation coefficients > 0.995). The detection limits for target compounds in this method ranged between 0.05 pmol L^{-1} and 0.50 pmol L^{-1} with a relative standard deviation of 3% to 9% (Table S1; He et al., 2013b, 2013c).

2.4 Determination of chlorophyll-*a* (Chl-*a*) in seawater

For the analysis of Chl-*a*, seawater samples (500 mL) were vacuum-filtered through a 0.7 μm Whatman GF/F glass fiber filter (diameter: 47 mm) and stored in the dark at -20 °C. Upon transport to the laboratory, the samples were extracted in the dark with 10 mL of 90% acetone for 24 h and centrifuged at 4000 rpm for 10 min. The supernatant was then analyzed using a fluorescence spectrophotometer (F-4500, Hitachi), achieving a detection limit of 0.01 μg L^{-1}.

2.5 Calculation of sea-air fluxes and saturation anomalies

The sea-air fluxes F (nmol m^{-2} d^{-1}) of VCHCs were calculated according to the following equation.

$$F = k_w (C_w - C_a/H) \quad (1)$$

where F (nmol m^{-2} d^{-1}) is the sea-air flux; k_w (m d^{-1}) is the gas exchange constant; C_w and C_a (pmol L^{-1}) are the concentrations of VCHCs in surface seawater and the atmosphere, respectively; and H is Henry's Law constant. Henry's Law constant was calculated based on the seawater temperature (T), where T is the Kelvin temperature. H values of $CHCl_3$, CCl_4, C_2HCl_3, and CH_3CCl_3 were obtained using the equations

https://doi.org/10.5194/egusphere-2025-251
Preprint. Discussion started: 24 February 2025

proposed by Schwardt et al. (2021):

$$H(CHCl_3) = \exp (164.98 - 10720\ T^{-1} - 22.98\ \mathrm{Ln}(T)) \quad (2)$$

$$H(CCl_4) = \exp (373.72 - 19941\ T^{-1} - 53.82\ \mathrm{Ln}(T)) \quad (3)$$

$$H(C_2HCl_3) = \exp (88.31 - 7242\ T^{-1} - 11.41\ \mathrm{Ln}(T)) \quad (4)$$

$$H(CH_3CCl_3) = \exp (459.80 - 23465\ T^{-1} - 66.96\ \mathrm{Ln}(T)) \quad (5)$$

k_w is calculated using the following equation by Wanninkhof (2014):

$$k_w = 0.251\ u^2\ (Sc / 660)^{-1/2} \quad (6)$$

where u is the wind speed and Sc is the Schmidt constant. The Sc values of VCHCs were calculated using the equation proposed by Khalil et al. (1999):

$$S_c = 335.6\ M^{1/2} \times (1 - 0.065\ t + 0.002043\ t^2 - 2.6 \times 10^{-5}\ t^3) \quad (7)$$

where t (°C) represents the temperature of the surface seawater and M is the molecular weight of VCHCs.

Saturation anomalies Δ (%) were calculated as the departure of the observed dissolved amount from equilibrium with air according to the following equation (Kurihara et al., 2010).

$$\Delta\% = 100\ (C_w - C_a/H) / C_a/\mathrm{H} \quad (8)$$

A positive saturation anomaly implies a net flux from the ocean to the air.

The uncertainty of the sea-air fluxes obtained in this study arises from both systematic and random measurement errors. Propagation of error analysis was conducted to quantify the uncertainty of the calculated sea-air fluxes, following the method outlined by Shoemaker et al. (1974).

$$\sigma^2 F = \left(\frac{\partial F}{\partial k_w}\right)^2 (\sigma k_w)^2 + \left(\frac{\partial F}{\partial C_w}\right)^2 (\sigma C_w)^2 + \left(\frac{\partial F}{\partial C_a}\right)^2 (\sigma C_a)^2 + \left(\frac{\partial F}{\partial H}\right)^2 (\sigma H)^2 \quad (9)$$

The precision of VCHCs measurements was under 9%, determined based on repeated sample injections. The overall error was calculated at approximately 20%, primarily due to the value of 20% from Wanninkhof (2014) for uncertainty in k_w,

https://doi.org/10.5194/egusphere-2025-251
Preprint. Discussion started: 24 February 2025

influenced by wind speed and *Sc* variabilities. Also, while a single Henry's Law calculation was done, there is uncertainty in both the determination of *H* and the temperature dependence. Thus, the error of the flux estimate in this study was determined to be > 20%.

2.6 Data analysis

The Hybrid Single Particle Lagrangian Integrated Trajectory (HYSPLIT) model, provided by the National Oceanic and Atmospheric Administration (NOAA) (http://www.arl.noaa.gov/ready.php), was employed to generate 96 h backward trajectories for air masses. The Matlab software was used to compile and analyze all survey station back trajectories. The TrajStat module for the MeteoInfo software was applied for trajectory analysis, enabling the clustering of trajectories based on geographic origins and historical paths identified in a previous study (Squizzato and Masiol, 2015). Following convention (Byčenkienė et al., 2014; Liu et al., 2017), these trajectories were initialized 100 m above sea level. Meteorological data were obtained from the Global Data Assimilation System (GDAS) dataset (http://ready.arl.noaa.gov/archives.php).

3 Results and discussion

3.1 Variability of the overlying atmospheric VCHCs concentrations

The variabilities in the atmospheric mixing ratios of the four VCHCs over the Western Pacific are detailed in Fig. 2 and Fig. 3. The results indicated that the distributions of the selected VCHCs were correlated with source strength and prevailing meteorological conditions. To better understand the fluctuations in their tropospheric concentrations, their sources, and their distribution patterns, we categorized the trace gases into two groups based on their molecular lifetimes (Table S1): (1) CCl_4 and CH_3CCl_3; (2) $CHCl_3$ and C_2HCl_3.

https://doi.org/10.5194/egusphere-2025-251
Preprint. Discussion started: 24 February 2025

3.1.1 CCl_4 and CH_3CCl_3

The atmospheric concentrations of CCl_4 and CH_3CCl_3 over the Western Pacific varied from 75.8 to 83.7 pptv (mean: 78.8 pptv) and from 1.6 to 2.4 pptv (mean: 2.0 pptv), respectively. The concentration of CCl_4 measured in the current work was similar to the average background mixing ratio of 78.5 pptv in the Northern Hemisphere during a survey from October 2019 to January 2020, as reported by AGAGE network (https://agage.mit.edu/). However, the concentration was considerably lower than the concentrations reported by Blake et al. (2003) for the Northwest Pacific Ocean (108.7 pptv) from February 24 to April 10, 2001, the measurements by Zhang et al. (2010) in 2007 for the Pearl River Delta region (116 pptv), those by Ou-Yang et al. (2017) in 2015 for the Mt. Fuji Research Station in Japan (84 pptv), and by Zheng et al. (2019) in 2015 at the Yellow River delta in China (109 pptv). The atmospheric concentration of CH_3CCl_3 in the investigated area was higher than the average background mixing ratio of 1.67 pptv in the Northern Hemisphere during a survey from October 2019 to January 2020 (https://agage.mit.edu/). However, the level reported here was lower than the concentration reported by He et al. (2013c) for the East China Sea (9.1 pptv) from May 2 to 9, 2012. Similarly, it was considerably lower than those reported by Blake et al. (2003) for the Northwest Pacific Ocean (132 pptv) from February 24 to April 10, 2001. It was also lower than the observed concentrations in the Pearl River Delta region (53 pptv) from October 25 to December 1, 2007, by Zhang et al. (2010); the Mt. Fuji Research Station in Japan (4.0 pptv) from August 12 to August 17, 2015, by Ou-Yang et al. (2017); and the Yellow River Delta region, northern China (2.8 pptv) from June 8 to July 9, 2017, by Zheng et al. (2019). Overall, the differences between our findings and previous measurements could be attributed primarily to temporal

https://doi.org/10.5194/egusphere-2025-251
Preprint. Discussion started: 24 February 2025

variability in emissions and changes in the global burden. Furthermore, the observed differences were partially due to the differences in the sampling locations. The samples were collected in a region minimally influenced by continental air masses, resulting in lower concentrations compared to areas closer to land.

Figure 3 illustrates the spatial distributions of atmospheric mixing ratios of CCl_4 and CH_3CCl_3. In the east-west direction, elevated concentrations of CCl_4 and CH_3CCl_3 were observed at the western monitoring stations (e.g., stations E130-15 and E130-18). These observation stations were situated near the Philippines and potentially influenced by coastal industrial production and domestic emissions. However, despite reports of high land-based emissions of CCl_4 (Liang et al., 2016; Sherry et al., 2018) and that CCl_4 was the second-most used feedstock chemical in mass production in 2019 (WMO, 2022), there is currently no evidence indicating significant CCl_4 emissions from the Philippines. Similarly, high levels of CCl_4 and CH_3CCl_3 were evident near mainland, particularly at the coastal stations (e.g., stations P1-1 to P1-7 and EQ12) in the north-south direction. Ni et al. (2023) observed relatively high atmospheric concentrations of SF_6 (anthropogenic sources) at the same stations. Furthermore, these findings aligned with numerous previous studies that reported elevated levels of CCl_4 and CH_3CCl_3 concentrated primarily in coastal areas (Blake et al., 2003; Zhang et al., 2010). These heightened concentrations could be attributed to the influence of polluted air masses from the mainland. In our study, the highest concentrations of CCl_4 and CH_3CCl_3 were recorded at station P1-4 near Japan. Utilizing backward trajectory clustering analysis (Fig. 4 and Fig. S3), it was determined that station P1-4 was affected by the short-distance transport of air masses from the eastern coast of Japan, which accounted for 13% of all contributing air masses. Long-distance transport of air masses from northeast China was also

https://doi.org/10.5194/egusphere-2025-251
Preprint. Discussion started: 24 February 2025

identified as a significant contributor to atmospheric CCl_4 and CH_3CCl_3 levels in this region, constituting approximately 72% of all air masses. Previous studies have indicated that atmospheric CCl_4 and CH_3CCl_3 were primarily from anthropogenic sources (Wang et al., 1995; Rigby et al., 2014). Liang et al. (2016) and Sherry et al. (2018) suggested that the emissions of CCl_4 from non-feedstock usage production are associated with chloromethane and perchloroethylene manufacturing facilities. Furthermore, as noted in the introduction, unreported and unintentional CCl_4 emissions from chlorine production and bleaching applications could contribute up to 10 Gg yr^{-1} (Liang et al., 2016; Sherry et al., 2018). Moreover, Zheng et al. (2019) and Ou-Yang et al. (2016) found that higher levels of CCl_4 and CH_3CCl_3 occurred in China and Japan, respectively. Lunt et al. (2018) also found continued emissions of CCl_4 from Eastern Asia. Therefore, the polluted air masses from Japan and China were likely responsible for the high CCl_4 and CH_3CCl_3 concentration at station P1-4 during the investigated period. In contrast, the lowest CCl_4 and CH_3CCl_3 concentrations were observed at station P1-24, where all affecting air mass trajectories came from the Pacific Ocean (Fig. 4 and Fig. S3). This indicated the low atmospheric CCl_4 and CH_3CCl_3 concentrations at this station were mainly attributed to clean air masses from the open ocean (Fig. 4).

3.1.2 $CHCl_3$ and C_2HCl_3

The atmospheric mixing ratios of $CHCl_3$ and C_2HCl_3 over the Western Pacific ranged from 6.0 to 29.4 pptv (mean: 12.4 ± 5.7 pptv) and from 1.1 to 3.4 pptv (mean: 2.0 ± 0.7 pptv), respectively. The concentration of $CHCl_3$ measured in the current work was similar to the average background mixing ratio of 11.82 pptv measured in the Northern Hemisphere during the survey period from October 2019 to January 2020, as reported by AGAGE network (https://agage.mit.edu/). The measured

https://doi.org/10.5194/egusphere-2025-251
Preprint. Discussion started: 24 February 2025

atmospheric concentration of $CHCl_3$ in the study area was lower than other areas, such as in a Northwest Pacific marginal sea—the South Yellow Sea—from May 2 to 9, 2012 (27.3 pptv; He et al., 2013c), the Mt. Fuji Research station of Japan from August 12 to August 17, 2015 (39 ± 11 pptv; Ou-Yang et al., 2017), and the Yellow River Delta region, northern China, from June 8 to July 9, 2017 (283 pptv; Zheng et al., 2019). The measurements of C_2HCl_3 were lower than in areas close to land sources, such as the South Yellow Sea from May 2 to 9, 2012 (27.3 pptv; He et al., 2013c) and the Yellow River Delta region, northern China, from June 8 to July 9, 2017 (20 pptv; Zheng et al., 2019). This difference could be attributed to the surveyed area being a relatively open sea, where the dilution effect by air from the marine boundary layer (MBL) is more pronounced. Furthermore, the air in the study area is more photochemically aged, leading to lower observed values of C_2HCl_3.

The atmospheric mixing ratios of $CHCl_3$ and C_2HCl_3 at the sampling stations are plotted in Fig. 2 and Fig. 3. High atmospheric mixing ratios of $CHCl_3$ and C_2HCl_3 were observed near the KEO areas and stations of EQ12, E130-15, and E130-18 (Fig. 3). The mixing ratios of both $CHCl_3$ and C_2HCl_3 showed significant correlations with SF_6 in the study area ($r = 0.56$, $n = 38$, and $p < 0.01$ and $r = 0.54$, $n = 38$, and $p < 0.01$, respectively; Fig. S4). The result indicated that the high concentrations of these two gases in the atmosphere mainly originated from anthropogenic input, as SF_6 is an important indicator of terrigenous sources. Moreover, the 96 h backward trajectory clusters showed the KOE region could be affected by atmospheric transport from China, Korea, and Japan (Fig. 4). Feng et al. (2019) found a rapid increase in $CHCl_3$ emissions from China. An et al. (2023) showed that $CHCl_3$ emissions of China peaked at 193 Gg yr^{-1} in 2017, then decreased to 147 Gg yr^{-1} in 2018, where they remained stable through 2020. Ou-Yang et al. (2017), at the Mt. Fuji research station in Japan in

https://doi.org/10.5194/egusphere-2025-251
Preprint. Discussion started: 24 February 2025

2015, observed high atmospheric mixing ratios of $CHCl_3$ (39 ± 11 pptv). Moreover, the highest annual mean atmospheric $CHCl_3$ (43 ± 18 pptv) was observed in 2017 at Gosan station (GSN, 127.17°E, 33.28°N, 72 m above sea level, a regional baseline station, Jeju Island, South Korea; Fig. 1). Previous studies identified industrial emissions as important sources of $CHCl_3$ and C_2HCl_3 (Montzka and Reimann et al., 2011; Oram et al., 2017; Zheng et al., 2019). These findings suggested that high $CHCl_3$ and C_2HCl_3 could be influenced by terrigenous atmospheric air mass transport from China, Korea, and Japan. Moreover, elevated atmospheric $CHCl_3$ and C_2HCl_3 levels were also correlated with high Chl-*a* concentrations in the KEO area ($r = 0.92$, $n = 8$, and $p < 0.01$ and $r = 0.68$, $n = 7$, and $p < 0.05$; Fig. S5), indicating oceanic emissions were a potential source. Positive saturation anomalies of $CHCl_3$ and C_2HCl_3 (Fig. 5) confirmed their supersaturation in the surface seawater, further suggesting the migration of these two gases from the sea to the atmosphere. Previous studies showed substantial amounts of $CHCl_3$ and C_2HCl_3 are released from marine macroalgae and microalgae (Abrahamsson et al., 1995; Chuck et al., 2005; Ekdahl et al., 1998; Lim et al., 2018) and enter the atmosphere via sea-to-air diffusion. Figure 5 shows that saturation anomalies and sea-air fluxes of $CHCl_3$ and C_2HCl_3 in the KEO area were lower than in other areas. Additionally, we found significant linear correlations among the concentrations of C_2HCl_3, $CHCl_3$, CCl_4, and CH_3CCl_3 in the marine atmosphere (Fig. 6), suggesting that these compounds share similar sources and atmospheric processes. The concentrations of CCl_4, and CH_3CCl_3 are mainly influenced by terrestrial atmospheric transport (see Section 3.1.1). Meanwhile, the concentrations of C_2HCl_3, dissolved in surface seawater are relatively low (see Section 3.2). Therefore, these findings suggested that the ocean emissions of C_2HCl_3 and $CHCl_3$ may not significantly contribute to the variations in their atmospheric concentrations, with

https://doi.org/10.5194/egusphere-2025-251
Preprint. Discussion started: 24 February 2025

terrestrial transport being their most important source.

3.2 Variability of surface VCHCs concentrations in seawater

The average concentrations (and ranges) of $CHCl_3$, CCl_4, C_2HCl_3, and CH_3CCl_3 in the Western Pacific were 9.5 (ranging from 3.2 to 20.7) pmol L^{-1}, 2.1 (ranging from 1.7 to 2.6) pmol L^{-1}, 2.4 (ranging from 1.1 to 3.7) pmol L^{-1}, and 0.10 (ranging from 0.06 to 0.14) pmol L^{-1}, respectively. The concentrations of $CHCl_3$ in this study were lower than in the Southern Yellow Sea and East China Sea measured by Yang et al. (2015) (ranging from 5.02 to 233 pmol L^{-1}) and He et al. (2019) (ranging from 6.8 to 275.6 pmol L^{-1}, mean of 33.5 pmol L^{-1}), and estuaries and nearshore areas (ranging from 16.75 to 2982.07 pmol L^{-1}) in European estuarine regions (Christof et al., 2002). Compared to the results of Karlsson et al. (2008) (ranging from 7.3 to 8.3 pmol L^{-1} in the Baltic Sea) and Huybrechts et al. (2004) (average concentration was 213.64 pmol L^{-1} in the Scheldt estuary), the CCl_4 concentrations in this study were lower. The CCl_4 concentrations we observed fell within the ranges reported in the East China Sea by Yang et al. (2015) (0.39 to 8.73 pmol L^{-1}) and in the Southern Yellow Sea and East China Sea by He et al. (2013a) (0.05 to 4.47 pmol L^{-1}). However, the C_2HCl_3 concentration range in this study was lower than other reported regions, including the South Atlantic and Atlantic Ocean regions ranging from 12 to 49 pmol L^{-1} (Abrahamsson et al., 2004a), the East China Sea ranging from 2.78 to 83.33 pmol L^{-1} (He et al., 2013a), the Bohai Sea and North Yellow Sea during spring ranging from 10.48 to 97.49 pmol L^{-1} (He et al., 2017), the Southern Yellow Sea and East China Sea ranging from 1.0 to 40.1 pmol L^{-1} (He et al., 2019), and the Northern Yellow Sea and Bohai Sea ranging from 17.46 to 136.54 pmol L^{-1} (Wei et al., 2019). The concentrations of CH_3CCl_3 in the study area were lower than in Liverpool Bay, UK (ranging from 0.22 to 182.16 pmol L^{-1}; Bravo-Linares et al., 2007), European

https://doi.org/10.5194/egusphere-2025-251
Preprint. Discussion started: 24 February 2025

estuarine regions (ranging from 0.75 to 358.32 pmol L^{-1}; Christof et al., 2002), the East China Sea (ranging from 0.39 to 8.73 pmol L^{-1}; He et al., 2013a), and the Southern Yellow Sea and East China Sea (ranging from 0.31 to 4.81 pmol L^{-1}; Yang et al., 2015). Based on the results of this study, the concentrations of VCHCs in the open ocean region were lower than in coastal and estuarine areas. Several previous studies have observed that, due to anthropogenic emissions and other land-based inputs, as well as the biological action of algae in coastal areas, VCHCs concentrations were generally higher in nearshore areas compared to open ocean regions (Christof et al., 2002; Abrahamsson et al., 2004b; Bravo-Linares et al., 2007; Yang et al., 2015; Wei et al., 2019).

3.3 Regional characteristics of seawater VCHCs and their driving factors

The seawater distributions of $CHCl_3$, C_2HCl_3, CCl_4, and CH_3CCl_3 are shown in Fig. 2 and Fig. S1. Seawater $CHCl_3$, C_2HCl_3, CCl_4, and CH_3CCl_3 exhibited significant regional variability in the Western Pacific. Surface concentrations of $CHCl_3$, C_2HCl_3, CCl_4, and CH_3CCl_3 in the KOE region were notably higher than those in the NPSG and WPWP (Fig. 2 and Fig. S1).

3.3.1 Kuroshio-Oyashio Extension

The Kuroshio-Oyashio Extension (KOE) area is characterized by a complex hydrography, with sharp meridional gradients in temperature and salinity due to the convergence of the warm, saline Kuroshio Current and the cold, less saline Oyashio Current (Fig. 2 and Fig. S1). Moreover, the Kuroshio Current transports warm seawater northward, where it cools and blends with the nutrient-rich Oyashio Current (Wan et al., 2023; Xu et al., 2023). The resulting upward flux of nutrients induced by the mesoscale eddies from the Kuroshio and the Kuroshio Extension replenish the upper ocean in the KOE with a substantial nutrient supply (Fig. S2). This, in turn,

https://doi.org/10.5194/egusphere-2025-251
Preprint. Discussion started: 24 February 2025

enhances primary productivity in the surface seawater, as evidenced by the elevated Chl-*a* concentrations observed here (Fig. 2).

The higher surface concentrations of $CHCl_3$ and C_2HCl_3 found in the KOE region could be due to a combination of phytoplankton abundance, the transport of terrestrial air masses, and SST. Firstly, the elevated concentrations of $CHCl_3$ and C_2HCl_3, corresponding to high Chl-*a* concentrations in the KOE region (Fig. 2), could be indicative of the influence of emissions from phytoplankton. The study by Roy et al. (2011) indicated that the distribution of $CHCl_3$ in the ocean was influenced by phytoplankton abundance. Indeed, phytoplankton blooms are known to contribute to the production of $CHCl_3$ and C_2HCl_3, as suggested by previous studies (Abrahamsson et al., 1995; Chuck et al., 2005; Roy et al., 2011; Lim et al., 2018). Diatoms and prymnesiophytes have been identified as dominant marine microalgae species responsible for releasing $CHCl_3$ (Roy et al., 2011; Lim et al., 2018). Wang et al. (2022) identified diatoms and dinoflagellates as the predominant microalgae species in the Northwest Pacific Ocean, with diatoms in particular thriving in the eutrophic Oyashio region. Secondly, given the proximity of the KOE region to Japan, atmospheric $CHCl_3$ and C_2HCl_3 might have been augmented by inputs from long-distance land-based air masses originating from Japan, Korea, and China (as discussed in Section 3.1). Additionally, the lower SST in this region facilitated the dissolution of $CHCl_3$ and C_2HCl_3, while high atmospheric concentrations of these compounds from long-distance land transport could have helped to replenish the $CHCl_3$ and C_2HCl_3 in the surface seawater. However, the saturation anomalies of $CHCl_3$ and C_2HCl_3 were positive during this cruise, suggesting $CHCl_3$ and C_2HCl_3 in the study area were supersaturated (Fig. 5). Therefore, given the seawater saturation of $CHCl_3$ and C_2HCl_3 in the region, and their short atmospheric lifetimes (< 6 months; WMO, 2022), it was

https://doi.org/10.5194/egusphere-2025-251
Preprint. Discussion started: 24 February 2025

505 inferred that emissions from phytoplankton in situ could have a stronger impact on
506 seawater concentrations of $CHCl_3$ and C_2HCl_3 than terrestrial sources of atmospheric
507 inputs. In contrast to $CHCl_3$ and C_2HCl_3, CCl_4 and CH_3CCl_3 exhibited negative
508 saturation anomalies in the study area, indicating undersaturation. Previous studies
509 have established that CCl_4 and CH_3CCl_3 primarily originate from anthropogenic
510 sources (Wang et al., 1995; Rigby et al., 2014). Therefore, the elevated concentrations
511 of CCl_4 and CH_3CCl_3 in the KOE region (Fig. 2 and Fig. S1) might have been caused
512 by the long-distance transport of air masses from Japan, Korea, and China (as
513 discussed in Section 3.1). Moreover, the lower SST in the KOE region may facilitate
514 the dissolution of CCl_4 and CH_3CCl_3, thereby increasing their concentrations in these
515 regions. Additionally, Fig. 5 shows that CCl_4 and CH_3CCl_3 were undersaturated across
516 the study region, further indicating that atmospheric transport influenced their
517 concentrations in seawater. Of particular note were the small variations in atmospheric
518 concentrations of CCl_4 and CH_3CCl_3, with lower instantaneous fluxes observed at
519 certain locations in the KOE region (Fig. 7). These factors affected the extent to
520 which atmospheric concentrations impacted the concentrations of CCl_4 and CH_3CCl_3
521 in seawater. The lower instantaneous fluxes observed in the KOE region were mainly
522 due to lower wind speeds (less than 3.5 m/s; Fig. 7), but the monthly average wind
523 speeds in the study area in 2019 were above 5 m/s (except in July; Fig. S6). Therefore,
524 from a long-term perspective, the sustained undersaturation and negative emission
525 fluxes suggested that the ocean has absorbed more CCl_4 and CH_3CCl_3 over time,
526 potentially reducing the atmospheric concentrations of CCl_4 and CH_3CCl_3. This was
527 consistent with previous studies that emphasized the role of the ocean as a significant
528 sink for halocarbons (Wang et al., 1995; Rigby et al., 2014).

529 **3.3.2 North Pacific Subtropical Gyre**

https://doi.org/10.5194/egusphere-2025-251
Preprint. Discussion started: 24 February 2025

Subtropical ocean gyres are often likened to marine deserts because of their persistent nutrient depletion and low organism standing stocks. In the NPSG, the primary mechanism for nutrient replenishment is from below, primarily through vertical eddy diffusion (Gupta et al., 2022). In contrast to the KOE region, the NPSG region lies at the center of the subtropical gyre, predominantly influenced by the deep nutricline and characterized by elevated temperatures, salinity, and diminished nutrient contents (Fig. S2). Xu et al. (2023) reported that the subsurface layer between 10°N and 35°N in the NPSG experiences nutrient depletion. This is because the environmental conditions of the NPSG limit the upward flux of nutrients through vertical transport, leaving the surface waters chronically nutrient-deprived. Fig. 2 and Fig. S1 show that concentrations of $CHCl_3$, C_2HCl_3, CCl_4, and CH_3CCl_3 in the NPSG were significantly lower than in the KOE, possibly because the NPSG is located far from land and has a high SST (Fig. 2). Additionally, the Chl-*a* levels and nutrients were considerably lower in the NPSG than the KOE region (Fig. S2). This suggested that the reduced release of $CHCl_3$ and C_2HCl_3 from phytoplankton could have also contributed to the lower concentrations of these gases observed in the NPSG. The lower nutrient levels in the NPSG lead to reduced phytoplankton biomass, resulting in lower production and release of halocarbons (Smythe-Wright et al., 2010; Liu et al., 2021).

3.3.3 Western Pacific Warm Pool

The concentrations of seawater $CHCl_3$ and C_2HCl_3 in the WPWP were similar to those in the NPSG (Fig. 2 and Fig. S1). Xu et al. (2023) proposed that this similarity could be because the WPWP region has a strong barrier layer, i.e., the layer of water between the isothermal layer and the mixed layer. In the WPWP, heavy precipitation enhances density stratification in the surface layers, resulting in a shallow mixed layer

https://doi.org/10.5194/egusphere-2025-251
Preprint. Discussion started: 24 February 2025

and a substantial barrier layer (Qu and Meyers, 2005). Despite the subsurface layer containing an abundance of nutrients, the presence of a robust barrier layer hinders the upward transport of nutrients and organic matter in the WPWP area (Fig. S2). This, combined with the high SST in this region (Fig. S2), might result in low surface concentrations of $CHCl_3$ and C_2HCl_3 in the WPWP region. Moreover, as shown in Fig. S1, higher concentrations of CCl_4 and CH_3CCl_3 were detected at stations closer to land in the WPWP. This might have been primarily due to the proximity of the WPWP to land (Papua New Guinea), where the input of CCl_4 from terrestrial sources through land runoff and terrestrial atmospheric transport (Fig. 4) could increase its concentration in surface seawater.

3.3.4 Correlations between VCHCs in seawater

$CHCl_3$ and C_2HCl_3 were found to be supersaturated in seawater, with previous studies suggesting that they primarily originate from biological processes within the ocean rather than relying solely on atmospheric inputs (see Section 3.3.1). The strong positive correlation between $CHCl_3$ and C_2HCl_3 in seawater ($r = 0.67$, $p < 0.01$; Fig. 7) supported the idea that these compounds share a common production mechanism, specifically emissions from biological processes. In contrast, CCl_4 and CH_3CCl_3 were undersaturated in seawater and primarily entered the ocean through atmospheric deposition, meaning that their concentrations in seawater were more influenced by atmospheric inputs (see Section 3.3.1). In addition, the correlation between CCl_4 and CH_3CCl_3 in seawater ($r = 0.43$, $p < 0.01$) was weaker than that between $CHCl_3$ and C_2HCl_3 (Fig. 6), which was likely due to the shorter lifetime and lower atmospheric concentration of CH_3CCl_3 compared to CCl_4 (Table S1; WMO, 2022). These results further confirmed that the distribution patterns of CCl_4 and CH_3CCl_3 in seawater were more influenced by atmospheric deposition, diffusion, and long-range transport.

https://doi.org/10.5194/egusphere-2025-251
Preprint. Discussion started: 24 February 2025

Moreover, despite the supersaturation of $CHCl_3$ and C_2HCl_3 in seawater and the undersaturation of CCl_4 and CH_3CCl_3, these four compounds still exhibited significant linear correlations in their concentrations (Fig. 7), suggesting that they were influenced by common oceanic and atmospheric processes. This correlation likely reflected partially overlapping sources, such as riverine input and atmospheric transport (Fogelqvist, 1985; He et al., 2013b). Additionally, oceanic physical processes, such as water mass mixing, diffusion, and vertical movement, played a crucial role in the distribution of gases in seawater (Doney et al., 2012). The synchronous influence of these processes on VCHCs might have been the reason for the linear correlation and similar distribution patterns observed for these four VCHCs in seawater. Specifically, in the Northwest Pacific, the unique hydrodynamic conditions significantly influenced the distribution patterns of $CHCl_3$, C_2HCl_3, CCl_4, and CH_3CCl_3 (Section 3.2). Major ocean currents, such as the Kuroshio and Oyashio, created zones of convergence and divergence that enhanced vertical and horizontal mixing, transporting gases from deeper waters to the surface and redistributing them across different regions, affecting their concentrations and distribution. Additionally, mesoscale eddies contribute to the diffusion of gases within the water column, resulting in gases from different sources (biogenic and atmospheric deposition) being more uniformly distributed in seawater (McGillicuddy, 2016; Xu et al., 2023).

3.4 Sea-air fluxes and saturation anomalies of VCHCs

The saturation anomalies and sea-air fluxes of $CHCl_3$, C_2HCl_3, CCl_4, and CH_3CCl_3 were estimated based on their simultaneously measured seawater and atmospheric concentrations, as outlined in Section 2.5 (Fig. 5 and Fig. 8). The saturation anomalies of $CHCl_3$ and C_2HCl_3 were positive, whereas CCl_4 and CH_3CCl_3 exhibited negative saturation anomalies at most stations of this study (Fig. 5).

https://doi.org/10.5194/egusphere-2025-251
Preprint. Discussion started: 24 February 2025

Moreover, the mean sea-air fluxes (range) for $CHCl_3$, C_2HCl_3, CCl_4, and CH_3CCl_3 were 21.2 (0.1–105.0), 6.8 (0.1–28.6), -0.9 (-6.3–0.0), and -0.1 (-0.3–0.2) nmol m^{-2} d^{-1}. These results indicated that $CHCl_3$ and C_2HCl_3 were in a state of supersaturation in the surface seawater, leading to their emission into the overlying atmosphere. In contrast, CCl_4 and CH_3CCl_3 were undersaturated within the surface seawater and were assimilated from the overlying atmosphere. Hence, we tentatively concluded that the Western Pacific was a source of $CHCl_3$ and C_2HCl_3 and a sink for CCl_4 and CH_3CCl_3 during the cruise periods. This has important implications for estimating the budgets of these VCHCs in the stratosphere and assessing their roles in stratospheric ozone depletion.

Compared to the marginal sea of the Northwest Pacific Ocean, this study's estimates of $CHCl_3$ and C_2HCl_3 emission and CCl_4 and CH_3CCl_3 uptake were lower (Yang et al., 2015; He et al., 2017; Wei et al., 2019). For example, the average flux of $CHCl_3$ and C_2HCl_3 in this study was significantly lower than those reported in the northern Yellow Sea and Bohai Sea by He et al. (2017) (C_2HCl_3: 162.6 nmol m^{-2} d^{-1}), Wei et al. (2019) ($CHCl_3$: 177.5 nmol m^{-2} d^{-1}, C_2HCl_3: 99.5 nmol m^{-2} d^{-1}), He et al. (2019) (C_2HCl_3: 59.4 nmol m^{-2} d^{-1}), and Yang et al. (2015) ($CHCl_3$: 183.4 nmol m^{-2} d^{-1}). Compared with the average fluxes of CCl_4 (-21.3 nmol m^{-2} d^{-1}) and CH_3CCl_3 (-6.8 nmol m^{-2} d^{-1}) in the South Yellow Sea and East China Sea as reported by Yang et al. (2015), the average fluxes of CCl_4 and CH_3CCl_3 in this study were lower. Although there were significant differences in sea-air fluxes compared with the marginal sea of the Northwest Pacific Ocean, both indicated that the ocean is a source of $CHCl_3$ and C_2HCl_3 in the atmosphere, but a sink of CCl_4 and CH_3CCl_3.

As shown in Fig. 8 and Fig. 9, the fluxes of $CHCl_3$ and C_2HCl_3 in the Western Pacific exhibited considerable spatial variability and generally corresponded with

https://doi.org/10.5194/egusphere-2025-251
Preprint. Discussion started: 24 February 2025

wind speeds. For instance, high fluxes of $CHCl_3$ and C_2HCl_3 at station P1-7 coincided with high wind speeds, while the low $CHCl_3$ and C_2HCl_3 fluxes at station E130-15 coincided with low wind speeds. However, as shown in Fig. 9, at a given wind speed, the fluxes were low due to low seawater concentrations of $CHCl_3$ and C_2HCl_3. Thus, seawater concentrations also had a large influence on the spatial variability of the sea-air fluxes of $CHCl_3$ and C_2HCl_3. The air-sea fluxes of CCl_4 and CH_3CCl_3 were also higher at stations with high wind speeds (Fig. 8 and Fig. S7). Similarly, Butler et al. (2016) found that the air-sea exchange rate was the primary driver of oceanic uptake of CCl_4, mainly driven by wind speed. However, the highest air-sea fluxes of CCl_4 and CH_3CCl_3 were observed at station P1-2, which had the highest equilibrium solubility (ratio of atmospheric concentration to Henry's Law constant) (Fig. 8). Moreover, at a given wind speed, the fluxes of CCl_4 and CH_3CCl_3 were lower where their atmospheric concentrations were lower and where SST was higher (Fig. S7 and Fig. S8). Therefore, the spatial variability of air-sea CCl_4 and CH_3CCl_3 fluxes were not only affected by wind speed but were also related to atmospheric CCl_4 and CH_3CCl_3 concentrations and SST. A similar investigation observed a comparable relationship between sea-air fluxes, wind speed, and atmospheric concentration while examining the distribution of SF_6 in seawater (Ni et al., 2023).

The annual absorption of CCl_4 in the Western Pacific (130°E–180°E, 0°–40°N) with an area of 2.17×10^7 km^2 was estimated to be 1.1 Gg yr^{-1}. The uncertainty associated with this extrapolation was quantified by constructing a 95% confidence interval using the standard error of the fluxes in the Western Pacific, while also considering the previously calculated uncertainty of > 20% in the flux estimates. The approximate estimate of annual absorption of CCl_4 ranged from 0.6 to 1.6 Gg yr^{-1}, with a total uncertainty of approximately 0.5 Gg yr^{-1}. The spatial variability in sea-air

https://doi.org/10.5194/egusphere-2025-251
Preprint. Discussion started: 24 February 2025

fluxes was caused by seasonal differences in CCl_4 atmospheric concentrations, SST, and wind speeds, which were also responsible for the uncertainty in this extrapolation. Based on the data from the AGAGE network (https://agage.mit.edu/), it was determined that the interannual variation in CCl_4 global atmospheric concentrations was about 2% in 2019, with interannual variability in CCl_4 for 2019 at the GSN of about 3% (Fig. S6a and b). In addition, the interannual variability of CCl_4 from October 2020 to September 2021 at the Shangdianzi (SDZ) background station in northern China (117.17°E, 40.65°N, 293 m above sea level; Fig. 1) was about 10% (Fig. S6c; Yi et al., 2023). Notably, the atmospheric concentrations of CCl_4 at the GSN and SDZ were higher than the annual average during the study period (Fig. S6b, S7c). Due to the influence of atmospheric transport from these regions, the observed atmospheric concentrations of CCl_4 in the Western Pacific may also have been higher than the annual average. Comparisons between atmospheric CCl_4 concentrations, SST, and wind speeds across different seasons revealed that atmospheric CCl_4 concentrations were higher during the study period, while wind speeds and SST remained near their annual averages (Fig. S6a; Tang et al., 2022). Based on these findings, the estimated annual uptake rate of CCl_4 by the Western Pacific in this study was likely to be higher. Additionally, considering that rising SST can reduce gas solubility, enhance ocean stratification, and alter wind patterns, absorption rates of CCl_4 by the ocean are likely to decrease. Therefore, we speculated that the increase in SST caused by global warming may weaken the ocean's ability to absorb CCl_4 in the future.

3.5 The role of western pacific in regulating Eastern Asia CCl_4

Eastern Asia, particularly eastern China, was a major source of global CCl_4 emissions, significantly contributing to the global CCl_4 burden (Lunt et al., 2018). The

https://doi.org/10.5194/egusphere-2025-251
Preprint. Discussion started: 24 February 2025

primary emission sources included the manufacture of general-purpose machinery, the production of CH_3Cl, CH_2Cl_2, $CHCl_3$, and C_2Cl_4, which generate CCl_4 as a byproduct, as well as the use of CCl_4 as a raw material and processing agent in the chemical manufacturing industry (Park et al., 2018, Li et al., 2024). Although CCl_4 emissions from eastern China declined significantly by nearly 45% between 2016 and 2019, Eastern Asia remained a major source of atmospheric CCl_4 (WMO, 2022). Our study showed that CCl_4 emissions from Eastern Asia were a significant source of atmospheric CCl_4 in the Northwestern Pacific (see section 3.1). The Western Pacific, as a sink for East Asian CCl_4, played a key role in regulating atmospheric CCl_4 concentrations. Based on our estimates (see section 3.4), the estimated oceanic absorption of CCl_4 in the Western Pacific (1.1 ± 0.5 Gg yr^{-1}) accounted for 17 ± 2% of the Eastern China emissions (6.3 ± 1.1 Gg yr^{-1} in 2019; WMO, 2022), 7 ± 5% of the emissions from Eastern Asia (16 (9–24) Gg yr^{-1} on average between 2009 and 2016; Lunt et al., 2018), and 3 ± 1% of the total global emissions (global emissions were 44 ± 14 Gg yr^{-1}; WMO, 2022). Furthermore, the estimated oceanic absorption of CCl_4 in the Western Pacific accounted for 8 ± 4% of the global oceanic absorption (14.4 Gg yr^{-1}; Butler et al., 2016). These data indicated that the Western Pacific as a sink of CCl_4 was crucial for regulating atmospheric CCl_4 concentrations and mitigating the accumulation of CCl_4 in atmosphere of Eastern Asia. This result was consistent with Butler et al. (2016), further confirming the critical role of the Western Pacific in the global CCl_4 cycle and emphasizing the ocean's indispensable role as a sink for atmospheric CCl_4. Notably, despite the estimate originating from a region with relatively little anthropogenic influence, the absorption capacity of the Western Pacific indicates it can significantly contribute to reducing global CCl_4 levels. This finding also aligned with Yvon-Lewis and Butler (2002), who demonstrated that

https://doi.org/10.5194/egusphere-2025-251
Preprint. Discussion started: 24 February 2025

oceans could effectively remove substantial quantities of CCl_4 from the atmosphere.

Additionally, a substantial body of prior data has indicated there is a CCl_4 deficit in deep ocean waters, especially in regions characterized by low oxygen levels (Krysell et al., 1994; Tanhua and Olsson, 2005). Recent studies have observed widespread undersaturation of CCl_4 in the surface waters of the Pacific, Atlantic, and Southern Oceans, suggesting the oceans consume a substantial amount of atmospheric CCl_4 and that biological sinks for CCl_4 may exist in the surface or near-surface waters of the oceans (Butler et al., 2016; Suntharalingam et al., 2019). These findings further supported the role of oceans as a CCl_4 sink and provided important insights for future oceanic environmental management and pollution control.

4 Conclusions

The present study reports the seawater and atmospheric concentrations, fluxes, sources, and control factors of VCHCs in the Western Pacific from 2019 to 2020. As seen from Figure 10, the presence or absence of upwelling, and whether the upwelling carries nutrients, and the transport of terrestrial inputs govern the biogeochemical characteristics of surface seawater in the Western Pacific, thereby influencing the concentrations and distributions of climatically relevant VCHCs. The measurements reported here indicated that the mesoscale eddies in the KOE region induced upwelling, bringing nutrient-rich subsurface water to the surface. This upwelling supplied ample nutrients to the surface seawater, fostering phytoplankton growth and organic matter photoreactions. These processes potentially enhanced the production of $CHCl_3$ and C_2HCl_3, resulting in high seawater concentrations of these compounds in the KOE. In contrast, the lower seawater concentrations of $CHCl_3$ and C_2HCl_3 in the NPSG and WPWP were attributed to the oligotrophic subsurface seawater in the NPSG and the suppression of upward nutrient and organic matter fluxes due to a

https://doi.org/10.5194/egusphere-2025-251
Preprint. Discussion started: 24 February 2025

robust barrier layer in the WPWP. The elevated seawater concentrations of CCl_4 and CH_3CCl_3 observed in the coastal area were caused by atmospheric inputs, seawater temperatures, and upwelling. These phenomena indicated that changes in marine environments, such as eddy activity, nutrient supply, and seasonal variations, can significantly impact VCHCs concentrations in seawater. Future research should focus on capturing a wider range of temporal and spatial variability to better understand these complex interactions. Atmospheric mixing ratios of CCl_4 and CH_3CCl_3 over the Western Pacific were predominantly determined by atmospheric inputs from Japan and Northeast China, as revealed through backward trajectory analysis. However, the atmospheric concentration of $CHCl_3$ and C_2HCl_3 in the study area were likely influenced by a combination of atmospheric transport from the continent and ocean emissions, with continental air mass transport potentially contributing more significantly. This preliminary estimation indicated that approximately 3 ± 1% of global CCl_4 emissions were absorbed by the Western Pacific. Our study also showed that 17 ± 2% of CCl_4 emitted from Eastern China and 7 ± 5% of Eastern Asia CCl_4 emissions could be absorbed by the Western Pacific, highlighting its crucial role in regulating atmospheric CCl_4 concentrations and mitigating accumulation in Eastern Asia atmosphere. In light of these findings, we tentatively propose that the capacity of the ocean to act as a sink for CCl_4 may warrant reevaluation. The global oceanic uptake of CCl_4 and CH_3CCl_3 and emissions of $CHCl_3$ and C_2HCl_3 could have influences on their global abundances and impact atmospheric chemistry.

Acknowledgments

We thank the chief scientists, captains, and crews of the R/V “Science” and “Dongfanghong 3” for their assistance and cooperation during the investigation. This work was funded by the National Natural Science Foundation of China (grant

https://doi.org/10.5194/egusphere-2025-251
Preprint. Discussion started: 24 February 2025

numbers 42276039 and 42406040) and Taishan Scholars Project Special Fund Support (tspd 20240805) and Postdoctoral Fellowship Program of CPSF (GZC20232705) and the Shandong Provincial Postdoctoral Foundation Project (Innovation Project) (SDCX-ZG-202400181) and the Qingdao Postdoctoral Applied Research Project (QDBSH20240101018). We thank the Institute of Oceanology, CAS, for samples and data from the NORC2019-09 cruise (NSFC grant 41849909) and the First Institute of Oceanography, MNR, for Chl-*a* data, with special thanks to Honghai Zhang of Ocean University of China for Chl-*a* data.

Data availability statement

The datasets containing wind speed, temperature, Chl-*a* concentrations, atmospheric and seawater concentrations of VCHCs, along with their saturation anomaly calculations and the estimated k_w for each flux measurement in the Western Pacific, are accessible via Figshare at https://doi.org/ 10.6084/m9.figshare.25639146.

Author contributions:

Shan-Shan Liu and Jie Ni designed the study, conducted VCHC measurements in the Western Pacific, analyzed the results, and contributed to manuscript writing. Xu-Xu Gao assisted with the observations. Jin-Ming Song reviewed and revised the manuscript. Zhen He interpreted the data and contributed to the manuscript. Gui-Peng Yang interpreted the analyzed results and reviewed and revised the manuscript.

Competing interests

The authors declare that they have no conflict of interest.

References

Abrahamsson, K., Bertilsson, S., Chierici, M., Fransson, A., Froneman, P. W., Lorén, A., & Pakhomov, E. A. (2004a). Variations of biochemical parameters along a transect in the Southern Ocean, with special emphasis on volatile halogenated

https://doi.org/10.5194/egusphere-2025-251
Preprint. Discussion started: 24 February 2025

organic compounds. Deep Sea Research Part II: Topical Studies in Oceanography, 51(22-24), 2745-2756.

Abrahamsson, K., Ekdahl, A., Collen, J., & Pedersen, M. (1995). Marine algae-a source of trichloroethylene and perchloroethylene. Limnology and Oceanography, 40(7), 1321-1326.

Abrahamsson, K., & Ekdahl, A. (1996). Volatile halogenated compounds and chlorophenols in the Skagerrak. Journal of Sea Research, 35(1-3), 73-79.

Abrahamsson, K., Lorén, A., Wulff, A., & Wängberg, S. Å. (2004b). Air-sea exchange of halocarbons: the influence of diurnal and regional variations and distribution of pigments. Deep Sea Research Part II: Topical Studies in Oceanography, 51(22-24), 2789-2805.

Adcock, K. E., Fraser, P. J., Hall, B. D., Langenfelds, R. L., Lee, G., Montzka, S. A., et al. (2021). Aircraft-based observations of ozone-depleting substances in the upper troposphere and lower stratosphere in and above the Asian summer monsoon. Journal of Geophysical Research: Atmospheres, 126(1), e2020JD033137.

An, M., Western, L. M., Say, D., Chen, L., Claxton, T., Ganesan, A. L., et al. (2021). Rapid increase in dichloromethane emissions from China inferred through atmospheric observations. Nature Communications, 12(1), 7279.

An, M., Western, L. M., Hu, J., Yao, B., Mühle, J., Ganesan, A. L., et al. (2023). Anthropogenic chloroform emissions from China drive changes in global emissions. Environmental Science & Technology, 57(37), 13925-13936.

Atlas, E., Pollock, W., Greenberg, J., Heidt, L., & Thompson, A. M. (1993). Alkyl nitrates, nonmethane hydrocarbons, and halocarbon gases over the equatorial

https://doi.org/10.5194/egusphere-2025-251
Preprint. Discussion started: 24 February 2025

Pacific Ocean during SAGA 3. Journal of Geophysical Research: Atmospheres, 98(D9), 16933-16947.

Blake, N. J., Blake, D. R., Simpson, I. J., Meinardi, S., Swanson, A. L., Lopez, J. P., et al. (2003). NMHCs and halocarbons in Asian continental outflow during the Transport and Chemical Evolution over the Pacific (TRACE-P) Field Campaign: Comparison with PEM-West B. Journal of Geophysical Research: Atmospheres, 108(D20).

Bravo-Linares, C. M., Mudge, S. M., & Loyola-Sepulveda, R. H. (2007). Occurrence of volatile organic compounds (VOCs) in Liverpool Bay, Irish Sea. Marine Pollution Bulletin, 54(11), 1742-1753.

Butler, J. H., Yvon-Lewis, S. A., Lobert, J. M., King, D. B., Montzka, S. A., Bullister, J. L., et al. (2016). A comprehensive estimate for loss of atmospheric carbon tetrachloride (CCl_4) to the ocean. Atmospheric Chemistry and Physics, 16(17), 10899-10910.

Byčenkienė, S., Dudoitis, V., & Ulevicius, V. (2014). The use of trajectory cluster analysis to evaluate the long-range transport of black carbon aerosol in the south-eastern Baltic region. Advances in Meteorology, 2014.

Carpenter, L. J., Reimann, S., Burkholder, J. B., Clerbaux, C., Hall, B. D., Hossaini, R., et al. (2014). Update on ozone-depleting substances (ODSs) and other gases of interest to the Montreal protocol. 9789966076014.

Chipperfield, M. P., Hossaini, R., Montzka, S. A., Reimann, S., Sherry, D., & Tegtmeier, S. (2020). Renewed and emerging concerns over the production and emission of ozone-depleting substances. Nature Reviews Earth & Environment, 1(5), 251-263.

Christof, O., Seifert, R., & Michaelis, W. (2002). Volatile halogenated organic

https://doi.org/10.5194/egusphere-2025-251
Preprint. Discussion started: 24 February 2025

compounds in European estuaries. Biogeochemistry, 59, 143-160.

Chuck, A. L., Turner, S. M., & Liss, P. S. (2005). Oceanic distributions and air-sea fluxes of biogenic halocarbons in the open ocean. Journal of Geophysical Research: Oceans, 110(C10).

Doney, S. C., Ruckelshaus, M., Emmett Duffy, J., Barry, J. P., Chan, F., English, C. A., et al. (2012). Climate change impacts on marine ecosystems. Annual review of marine science, 4(1), 11-37.

Ekdahl, A., Pedersén, M., & Abrahamsson, K. (1998). A study of the diurnal variation of biogenic volatile halocarbons. Marine Chemistry, 63(1-2), 1-8.

Fang, X., Park, S., Saito, T., Tunnicliffe, R., Ganesan, A. L., Rigby, M., et al. (2019). Rapid increase in ozone-depleting chloroform emissions from China. Nature Geoscience, 12(2), 89-93.

Fogelqvist, E. (1985). Carbon tetrachloride, tetrachloroethylene, 1, 1, 1-trichloroethane and bromoform in Arctic seawater. Journal of Geophysical Research: Oceans, 90(C5), 9181-9193.

Gschwend, P. M., MacFarlane, J. K., & Newman, K. A. (1985). Volatile halogenated organic compounds released to seawater from temperate marine macroalgae. Science, 227(4690), 1033-1035.

Gupta, M., Tripathi, N., Malik, T. G., & Sahu, L. K. (2024). A review on air–sea exchange of reactive trace gases over the northern Indian Ocean. Journal of Earth System Science, 133(2), 77.

Gupta, M., Williams, R. G., Lauderdale, J. M., Jahn, O., Hill, C., Dutkiewicz, S., & Follows, M. J. (2022). A nutrient relay sustains subtropical ocean productivity. Proceedings of the National Academy of Sciences, 119(41), e2206504119.

https://doi.org/10.5194/egusphere-2025-251
Preprint. Discussion started: 24 February 2025

He, Z., Liu, S. S., Ni, J., Chen, Y., & Yang, G. P. (2019). Spatio-temporal variability and sources of volatile halocarbons in the South Yellow Sea and the East China Sea. Marine Pollution Bulletin, 149, 110583.

He, Z., Yang, G. P., & Lu, X. L. (2013a). Distributions and sea-to-air fluxes of volatile halocarbons in the East China Sea in early winter. Chemosphere, 90(2), 747-757.

He, Z., Liu, Q. L., Zhang, Y. J., & Yang, G. P. (2017). Distribution and sea-to-air fluxes of volatile halocarbons in the Bohai Sea and North Yellow Sea during spring. Science of the Total Environment, 585, 546-553.

He, Z., Yang, G., Lu, X., & Zhang, H. (2013b). Distributions and sea-to-air fluxes of chloroform, trichloroethylene, tetrachloroethylene, chlorodibromomethane and bromoform in the Yellow Sea and the East China Sea during spring. Environmental Pollution, 177, 28-37.

He, Z., Yang, G. P., Lu, X. L., Ding, Q. Y., & Zhang, H. H. (2013c). Halocarbons in the marine atmosphere and surface seawater of the south Yellow Sea during spring. Atmospheric Environment, 80, 514-523.

Hersbach, H., Bell, B., Berrisford, P., Hirahara, S., Horányi, A., Muñoz-Sabater, J., et al. (2020). The ERA5 global reanalysis. Quarterly Journal of the Royal Meteorological Society, 146(730), 1999-2049.

Hossaini, R., Chipperfield, M. P., Saiz-Lopez, A., Harrison, J. J., von Glasow, R., Sommariva, R., et al. (2015). Growth in stratospheric chlorine from short-lived chemicals not controlled by the Montreal Protocol. Geophysical Research Letters, 42(11), 4573-4580.

Hossaini, R., Chipperfield, M. P., Montzka, S. A., Leeson, A. A., Dhomse, S. S., & Pyle, J. A. (2017). The increasing threat to stratospheric ozone from dichloromethane. Nature Communications, 8(1), 15962.

https://doi.org/10.5194/egusphere-2025-251
Preprint. Discussion started: 24 February 2025

878 Hu, D., Wang, F., Sprintall, J., Wu, L., Riser, S., Cravatte, S., et al. (2020). Review on
879 observational studies of western tropical Pacific Ocean circulation and climate.
880 Journal of Oceanology and Limnology, 38(4), 906-929.
881 Hu, D., Wu, L., Cai, W., Gupta, A. S., Ganachaud, A., Qiu, B., et al. (2015). Pacific
882 western boundary currents and their roles in climate. Nature, 522(7556),
883 299-308.
884 Huybrechts, T., Dewulf, J., & Van Langenhove, H. (2004). Spatial and temporal
885 variability of priority volatile organic compounds in the Scheldt estuary. Water
886 research, 38(14-15), 3241-3250.
887 Jiao, Y., Ruecker, A., Deventer, M. J., Chow, A. T., & Rhew, R. C. (2018). Halocarbon
888 emissions from a degraded forested wetland in coastal South Carolina impacted
889 by sea level rise. ACS Earth and Space Chemistry, 2(10), 955-967.
890 Karlsson, A., Auer, N., Schulz-Bull, D., & Abrahamsson, K. (2008). Cyanobacterial
891 blooms in the Baltic–A source of halocarbons. Marine Chemistry, 110(3-4),
892 129-139.
893 Khalil, M. A. K., Moore, R. M., Harper, D. B., Lobert, J. M., Erickson, D. J.,
894 Koropalov, V., et al. (1999). Natural emissions of chlorine-containing gases:
895 Reactive Chlorine Emissions Inventory. Journal of Geophysical Research:
896 Atmospheres, 104(D7), 8333-8346.
897 Khan, M. A. H., Rhew, R. C., Whelan, M. E., Zhou, K., & Deverel, S. J. (2011).
898 Methyl halide and chloroform emissions from a subsiding Sacramento–San
899 Joaquin Delta island converted to rice fields. Atmospheric Environment, 45(4),
900 977-985.

https://doi.org/10.5194/egusphere-2025-251
Preprint. Discussion started: 24 February 2025

Krysell, M., Fogelqvist, E., & Tanhua, T. (1994). Apparent removal of the transient tracer carbon tetrachloride from anoxic seawater. Geophysical Research Letters, 21(23), 2511-2514.

Kurihara, M. K., Kimura, M., Iwamoto, Y., Narita, Y., Ooki, A., Eum, Y J., et al. (2010). Distributions of short-lived iodocarbons and biogenic trace gases in the open ocean and atmosphere in the western North Pacific. Marine Chemistry, 118, 156-170.

Li, B., Huang, J., Hu, X., Zhang, L., Ma, M., Hu, L., et al., (2024). CCl_4 emissions in eastern China during 2021–2022 and exploration of potential new sources. Nature Communications, 15(1), 1725.

Li, J. L., Zhai, X., Ma, Z., Zhang, H. H., & Yang, G. P. (2019a). Spatial distributions and sea-to-air fluxes of non-methane hydrocarbons in the atmosphere and seawater of the Western Pacific. Science of the Total Environment, 672, 491-501.

Li, Y., He, Z., Yang, G. P., Wang, H., & Zhuang, G. C. (2019b). Volatile halocarbons in the marine atmosphere and surface seawater: diurnal and spatial variations and influences of environmental factors. Atmospheric Environment, 214, 116820.

Liang, Q., Newman, P. A., Daniel, J. S., Reimann, S., Hall, B. D., Dutton, G., & Kuijpers, L. J. (2014). Constraining the carbon tetrachloride (CCl_4) budget using its global trend and inter-hemispheric gradient. Geophysical Research Letters, 41(14), 5307-5315.

Liang, Q., Newman, P. A., & Reimann, S. (2016). SPARC report on the mystery of carbon tetrachloride. ETH Zurich，SPARC, Volume 7.

Lim, Y. K., Phang, S. M., Sturges, W. T., Malin, G., & Rahman, N. B. A., (2018). Emission of short-lived halocarbons by three common tropical marine microalgae during batch culture. Journal of Applied Phycolpgy, 30(1), 1-13.

https://doi.org/10.5194/egusphere-2025-251
Preprint. Discussion started: 24 February 2025

926 Liu, T., Gong, S., He, J., Yu, M., Wang, Q., Li, H., et al. (2017). Attributions of
927 meteorological and emission factors to the 2015 winter severe haze pollution
928 episodes in China's Jing-Jin-Ji area. Atmospheric Chemistry and Physics, 17(4),
929 2971-2980.
930 Liu, S. S., Yang, G. P., He, Z., Gao, X. X., & Xu, F. (2021). Oceanic emissions of
931 methyl halides and effect of nutrients concentration on their production: A case of
932 the Northwest Pacific (2°N to 24°N). Science of the Total Environment, 769,
933 144488.
934 Lunt, M. F., Park, S., Li, S., Henne, S., Manning, A. J., Ganesan, A. L., et al. (2018).
935 Continued emissions of the ozone-depleting substance carbon tetrachloride from
936 Eastern Asia. Geophysical Research Letters, 45(20), 11-423.
937 Mahajan, A. S., Shaw, M., Oetjen, H., Hornsby, K. E., Carpenter, L. J., Kaleschke, L.,
938 et al. (2010). Evidence of reactive iodine chemistry in the Arctic boundary layer.
939 Journal of Geophysical Research: Atmospheres, 115(D20).
940 McGillicuddy Jr, D. J. (2016). Mechanisms of physical-biological-biogeochemical
941 interaction at the oceanic mesoscale. Annual Review of Marine Science, 8(1),
942 125-159.
943 Menemenlis, D., Campin, J. M., Heimbach, P., Hill, C., Lee, T., Nguyen, A., et al.
944 (2008). ECCO2: High resolution global ocean and sea ice data synthesis.
945 Mercator Ocean Quarterly Newsletter, 31, 13-21 .
946 Montzka, S. A., Reimann, S., Engel, A., Krüger, K., O'Doherty, S., Sturges, W. T., et
947 al. (2011). Ozone depleting substances (ODS's) and related chemicals, Chapter 1
948 in: scientific assessment of ozone depletion: 2010. Global Ozone Research and
949 Monitoring Project. World Meteorological Organization, Geneva, Switzerland,
950 516, 1-112.

https://doi.org/10.5194/egusphere-2025-251
Preprint. Discussion started: 24 February 2025

Moore, R. M. (2003). Marine sources of volatile organohalogens. Natural Production of Organohalogen Compounds, 85-101.

Ni, J., Liu, S. S., Lang, X. P., He, Z., & Yang, G. P. (2023). Sulfur hexafluoride in the marine atmosphere and surface seawater of the Western Pacific and Eastern Indian Ocean. Environmental Pollution, 335, 122266.

Oram, D. E., Ashfold, M. J., Laube, J. C., Gooch, L. J., Humphrey, S., Sturges, W. T., et al. (2017). A growing threat to the ozone layer from short-lived anthropogenic chlorocarbons. Atmospheric Chemistry and Physics, 17(19), 11929-11941.

Ou-Yang, C. F., Chang, C. C., Wang, J. L., Shimada, K., Hatakeyama, S., Kato, S., et al. (2017). Characteristics of summertime volatile organic compounds in the lower free troposphere: Background measurements at Mt. Fuji. Aerosol and Air Quality Research, 17(12), 3037-3051.

Park, S., Li, S., Mühle, J., O'Doherty, S., Weiss, R. F., Fang, X., et al., (2018). Toward resolving the budget discrepancy of ozone-depleting carbon tetrachloride (CCl_4): an analysis of top-down emissions from China. Atmospheric Chemistry and Physics, 18(16), 11729-11738.

Plummer, J. D., & Edzwald, J. K. (2002). Effects of chlorine and ozone on algal cell properties and removal of algae by coagulation. Journal of Water Supply: Research and Technology-AQUA, 51(6), 307-318.

Qu, T., & Meyers, G. (2005). Seasonal variation of barrier layer in the southeastern tropical Indian Ocean. Journal of Geophysical Research: Oceans, 110(C11).

Quack, B., & Suess, E. (1999). Volatile halogenated hydrocarbons over the western Pacific between 43°N and 4°N. Journal of Geophysical Research: Atmospheres, 104(D1), 1663-1678.

https://doi.org/10.5194/egusphere-2025-251
Preprint. Discussion started: 24 February 2025

975 Rigby, M., Prinn, R. G., O'doherty, S., Miller, B. R., Ivy, D., Mühle, J., et al. (2014).
976 Recent and future trends in synthetic greenhouse gas radiative forcing.
977 Geophysical Research Letters, 41(7), 2623-2630.
978 Roy, R., Pratihary, A., Narvenkar, G., Mochemadkar, S., Gauns, M., & Naqvi, S. W. A.
979 (2011). The relationship between volatile halocarbons and phytoplankton
980 pigments during a Trichodesmium bloom in the coastal eastern Arabian Sea.
981 Estuarine, Coastal and Shelf Science, 95(1), 110-118.
982 Saiz-Lopez, A., Fernandez, R. P., Li, Q., Cuevas, C. A., Fu, X., Kinnison, D. E., et al.
983 (2023). Natural short-lived halogens exert an indirect cooling effect on climate.
984 Nature, 618(7967), 967-973.
985 Say, D., Kuyper, B., Western, L., Khan, M. A. H., Lesch, T., Labuschagne, C., et al.
986 (2020). Emissions and marine boundary layer concentrations of unregulated
987 chlorocarbons measured at Cape Point, South Africa. Environmental Science &
988 Technology, 54(17), 10514-10523.
989 Scarratt, M. G., & Moore, R. M. (1999). Production of chlorinated hydrocarbons and
990 methyl iodide by the red microalga Porphyridium purpureum. Limnology and
991 Oceanography, 44(3), 703-707.
992 Schwardt, A., Dahmke, A., & Köber, R. (2021). Henry's law constants of volatile
993 organic compounds between 0 and 95 °C–Data compilation and
994 complementation in context of urban temperature increases of the subsurface.
995 Chemosphere, 272, 129858.
996 Shechner, M., Guenther, A., Rhew, R., Wishkerman, A., Li, Q., Blake, D., et al.
997 (2019). Emission of volatile halogenated organic compounds over various Dead
998 Sea landscapes. Atmospheric Chemistry and Physics, 19(11), 7667-7690.
999 Sherry, D., McCulloch, A., Liang, Q., Reimann, S., & Newman, P. A. (2018). Current

https://doi.org/10.5194/egusphere-2025-251
Preprint. Discussion started: 24 February 2025

sources of carbon tetrachloride (CCl_4) in our atmosphere. Environmental Research Letters, 13(2), 024004.

Shi, J., Jia, Q., Nürnberg, D., Li, T., Xiong, Z., & Qin, B. (2022). Coupled nutricline and productivity variations during the Pliocene in the western Pacific warm pool and their paleoceanographic implications. Global and Planetary Change, 212, 103810.

Squizzato, S., & Masiol, M. (2015). Application of meteorology-based methods to determine local and external contributions to particulate matter pollution: A case study in Venice (Italy). Atmospheric Environment, 119, 69-81.

Suntharalingam, P., Buitenhuis, E., Carpenter, L. J., Butler, J. H., Messias, M. J., Andrews, S. J., & Hackenberg, S. C. (2019). Evaluating oceanic uptake of atmospheric CCl_4: A combined analysis of model simulations and observations. Geophysical Research Letters, 46(1), 472-482.

Smythe-Wright, D., Peckett, C., Boswell, S., & Harrison, R. (2010). Controls on the production of organohalogens by phytoplankton: Effect of nitrate concentration and grazing. Journal of Geophysical Research: Biogeosciences, 115(G3).

Tanhua, T., & Olsson, K. A. (2005). Removal and bioaccumulation of anthropogenic, halogenated transient tracers in an anoxic fjord. Marine chemistry, 94(1-4), 27-41.

Tang, C., Tao, X., Wei, Y., Tong, Z., Zhu, F., & Lin, H. (2022). Analysis and prediction of wind speed effects in East Asia and the Western Pacific based on multi-source data. Sustainability, 14(19), 12089.

Treadaway, V., Atlas, E., Schauffler, S., Navarro, M., Ueyama, R., Pfister, L., et al. (2022). Long-range transport of Asian emissions to the West Pacific tropical tropopause layer. Journal of Atmospheric Chemistry, 79(2), 81-100.

https://doi.org/10.5194/egusphere-2025-251
Preprint. Discussion started: 24 February 2025

Tsunogai, S. (2002). The western North Pacific playing a key role in global biogeochemical fluxes. Journal of Oceanography, 58, 245-257.

Wan, S., Xiang, R., Steinke, S., Du, Y., Yang, Y., Wang, S., & Wang, H. (2023). Impact of the Western Pacific Warm pool and Kuroshio dynamics in the Okinawa Trough during the Holocene. Global and Planetary Change, 224, 104116.

Wang, J. L., Blake, D. R., & Rowland, F. S. (1995). Seasonal variations in the atmospheric distribution of a reactive chlorine compound, tetrachloroethene (CCl_2=CCl_2). Geophysical Research Letters, 22(9), 1097-1100.

Wang, B., Kang, I. S., & Lee, J. Y. (2004). Ensemble simulations of Asian–Australian monsoon variability by 11 AGCMs. Journal of Climate, 17(4), 803-818.

Wang, Y., Bi, R., Zhang, J., Gao, J., Takeda, S., Kondo, Y., et al. (2022). Phytoplankton distributions in the Kuroshio-Oyashio Region of the Northwest Pacific Ocean: Implications for marine ecology and carbon cycle. Frontiers in Marine Science, 9, 865142.

Wanninkhof, R. (2014). Relationship between wind speed and gas exchange over the ocean revisited. Limnology & Oceanography: Methods, 12, 351-362.

Wei, Y., He, Z., & Yang, G. P. (2019). Seasonal and spatial variations of chloroform, trichloroethylene, tetrachloroethylene, chlorodibromomethane and bromoform in the Northern Yellow Sea and Bohai Sea. Environmental Chemistry, 16(2), 114-124.

WMO (World Meteorological Organization). (2018). Scientific Assessment of Ozone Depletion: 2018. Global Ozone Research and Monitoring Project-Report No. 58, 588 pp, Geneva, Switzerland.

WMO (World Meteorological Organization). (2022). Scientific Assessment of Ozone

https://doi.org/10.5194/egusphere-2025-251
Preprint. Discussion started: 24 February 2025

Depletion 2022. Global Ozone Research and Monitoring Project-Report No. 278, 509 pp, Geneva, Switzerland.

Xu, F., Zhang, H. H., Yan, S. B., Sun, M. X., Wu, J. W., & Yang, G. P. (2023). Biogeochemical controls on climatically active gases and atmospheric sulfate aerosols in the western Pacific. Environmental Research, 220, 115211.

Yang, G. P., Li, L., Lu, X. L., & Zhang, L. (2015). Distributions and sea-to-air fluxes of volatile halocarbons in the southern Yellow Sea and the East China Sea. Acta Oceanologica Sinica, 34(2), 9-20.

Yi, L., An, M., Yu, H., M, Z., Xu, L., O'Doherty, S., et al. (2023). In Situ Observations of Halogenated Gases at the Shangdianzi Background Station and Emission Estimates for Northern China. Environmental Science & Technology, 57(18), 7217-7229.

Yokouchi, Y., Inagaki, T., Yazawa, K., Tamaru, T., Enomoto, T., & Izumi, K. (2005). Estimates of ratios of anthropogenic halocarbon emissions from Japan based on aircraft monitoring over Sagami Bay, Japan. Journal of Geophysical Research: Atmospheres, 110(D6).

Yuan, D., He, Z., & Yang, G. P. (2019). Spatiotemporal distributions of halocarbons in the marine boundary air and surface seawater of the Changjiang estuary and its adjacent East China Sea. Marine Pollution Bulletin, 140, 227-240.

Yu, D., Yao, B., Lin, W., Vollmer, M. K., Ge, B., Zhang, G., et al. (2020). Atmospheric CH_3CCl_3 observations in China: Historical trends and implications. Atmospheric Research, 231, 104658.

Zhang, Y. L., Guo, H., Wang, X. M., Simpson, I. J., Barletta, B., Blake, D. R., et al. (2010). Emission patterns and spatiotemporal variations of halocarbons in the Pearl River Delta region, southern China. Journal of Geophysical Research:

https://doi.org/10.5194/egusphere-2025-251
Preprint. Discussion started: 24 February 2025

Atmospheres, 115(D15).

Zhang, W., Jiao, Y., Zhu, R., Rhew, R. C., Sun, B., & Dai, H. (2021). Chloroform ($CHCl_3$) emissions from coastal Antarctic tundra. Geophysical Research Letters, 48(18), e2021GL093811.

Zheng, P., Chen, T., Dong, C., Liu, Y., Li, H., Han, G., et al. (2019). Characteristics and sources of halogenated hydrocarbons in the Yellow River Delta region, northern China. Atmospheric Research, 225, 70-80.

https://doi.org/10.5194/egusphere-2025-251
Preprint. Discussion started: 24 February 2025

FIGURE CAPTIONS

Fig. 1. (A) Locations of sampling stations (SDZ: Shangdianzi background station; GSN: Gosan station). The VCHCs data for the GSN were obtained from AGAGE network (https://agage.mit.edu/) and the VCHCs data for the SDZ were derived from Yi et al. (2023). (B) A schematic map of the major currents (KOE: Kuroshio-Oyashio Extension; NPSG: North Pacific Subtropical Gyre; WPWP: Western Pacific Warm Pool; OC: Oyashio Current; KC: Kuroshio Current; KE: Kuroshio Extension; NEC: North Equatorial Current; NEUC: North Equatorial Undercurrent; NECC: North Equatorial Countercurrent; EUC: Equatorial Undercurrent; SEC: South Equatorial Current; MC: Mindanao Current; NGCC: New Guinea Coastal Current; ME: Mindanao Eddy and; HE: Halmahera Eddy).

Fig. 2. Latitudinal distributions of surface seawater of temperature, salinity, and Chl-*a*, and surface seawater and atmospheric concentrations of $CHCl_3$, CCl_4, C_2HCl_3, and CH_3CCl_3, along with wind speed in the Western Pacific.

Fig. 3. Distributions of $CHCl_3$, CCl_4, C_2HCl_3, and CH_3CCl_3 in the marine atmospheric boundary layer of the Western Pacific.

Fig. 4. Clusters of 96 h backward trajectories for different stations over the Western Pacific. The ensembled 96 h back-trajectories were within the lower troposphere above 10 m (red lines), above 100 m (black lines), and above 1000 m (green lines).

Fig. 5. Saturation anomaly of $CHCl_3$, CCl_4, C_2HCl_3, and CH_3CCl_3 in the Western Pacific.

Fig. 6. Relationships between $CHCl_3$, CCl_4, C_2HCl_3, and CH_3CCl_3 in the atmosphere of the Western Pacific.

Fig. 7. Relationships between $CHCl_3$, CCl_4, C_2HCl_3, and CH_3CCl_3 in the seawater of the Western Pacific.

https://doi.org/10.5194/egusphere-2025-251
Preprint. Discussion started: 24 February 2025

Fig. 8. Sea-air fluxes of $CHCl_3$, CCl_4, C_2HCl_3, and CH_3CCl_3, along with wind speeds in the Western Pacific.

Fig. 9. Relationships between the sea-air fluxes of $CHCl_3$ (a) and C_2HCl_3 (b) and wind speed and seawater concentrations of $CHCl_3$ and C_2HCl_3 (points are colored according to seawater concentrations).

Fig. 10. Schematic diagram of key processes and factors controlling the production and distributions, as well as the sea-air interactions, of VCHCs in the Western Pacific.

https://doi.org/10.5194/egusphere-2025-251
Preprint. Discussion started: 24 February 2025

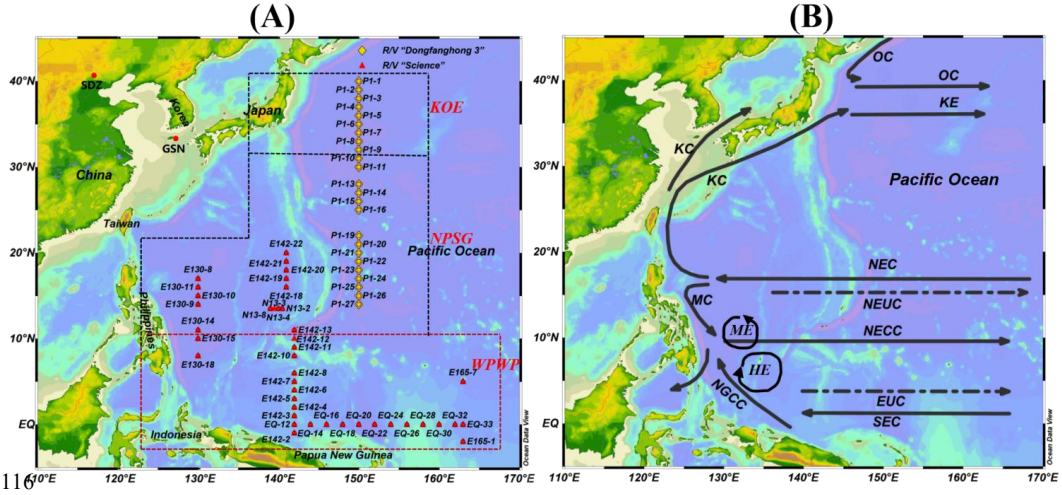

Fig. 1. (A) Locations of sampling stations (SDZ: Shangdianzi background station; GSN: Gosan station). The VCHCs data for the GSN were obtained from AGAGE network (https://agage.mit.edu/) and the VCHCs data for the SDZ were derived from Yi et al. (2023). (B) A schematic map of the major currents (KOE: Kuroshio-Oyashio Extension; NPSG: North Pacific Subtropical Gyre; WPWP: Western Pacific Warm Pool; OC: Oyashio Current; KC: Kuroshio Current; KE: Kuroshio Extension; NEC: North Equatorial Current; NEUC: North Equatorial Undercurrent; NECC: North Equatorial Countercurrent; EUC: Equatorial Undercurrent; SEC: South Equatorial Current; MC: Mindanao Current; NGCC: New Guinea Coastal Current; ME: Mindanao Eddy and; HE: Halmahera Eddy).

https://doi.org/10.5194/egusphere-2025-251
Preprint. Discussion started: 24 February 2025

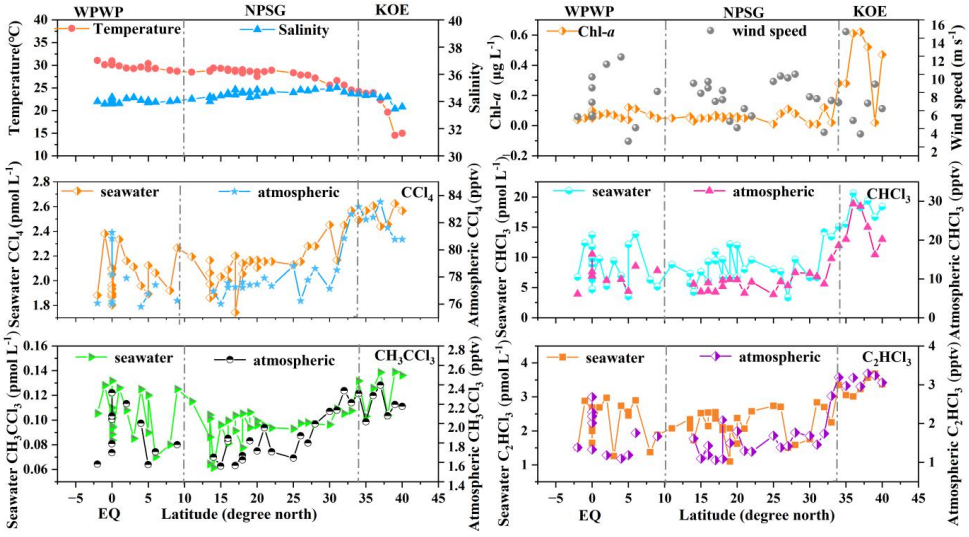

Fig. 2. Latitudinal distributions of surface seawater of temperature, salinity, and Chl-*a*, and surface seawater and atmospheric concentrations of $CHCl_3$, CCl_4, C_2HCl_3, and CH_3CCl_3, along with wind speed in the Western Pacific.

https://doi.org/10.5194/egusphere-2025-251
Preprint. Discussion started: 24 February 2025

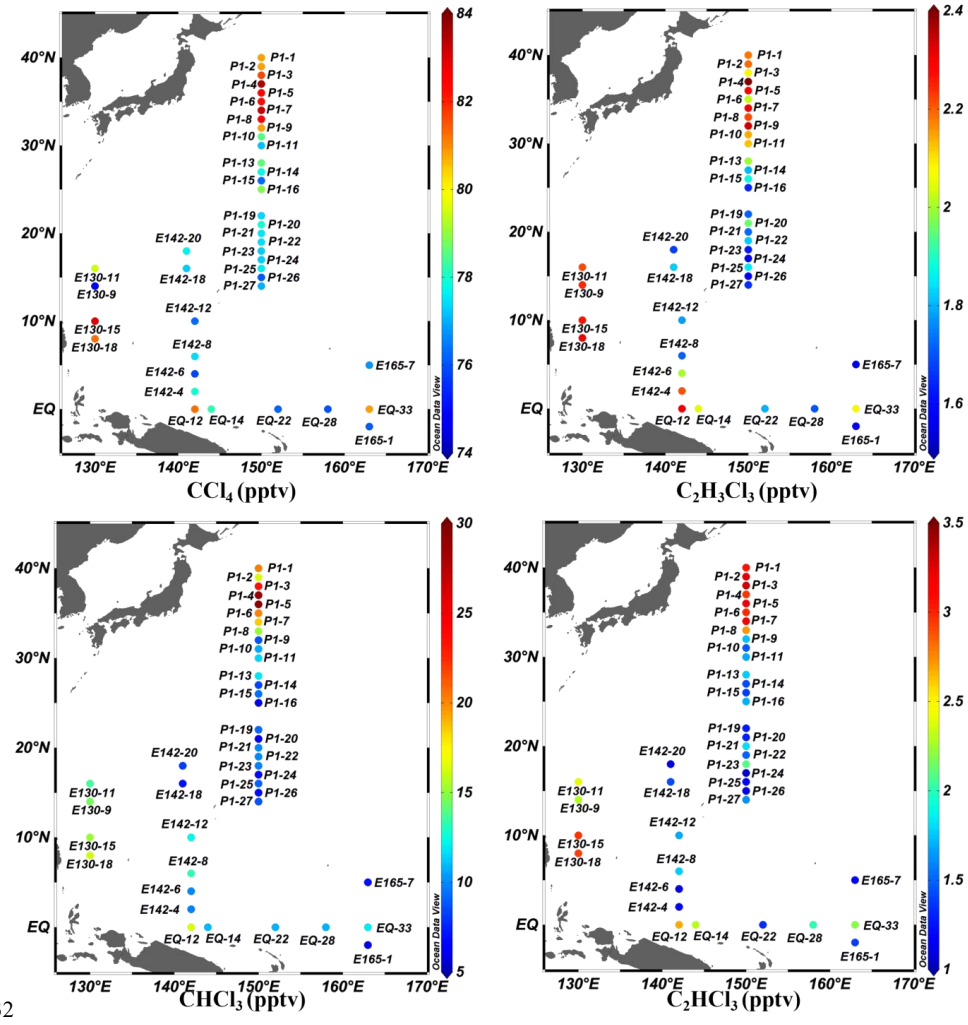

Fig. 3. Distributions of $CHCl_3$, CCl_4, C_2HCl_3, and CH_3CCl_3 in the marine atmospheric boundary layer of the Western Pacific.

https://doi.org/10.5194/egusphere-2025-251
Preprint. Discussion started: 24 February 2025

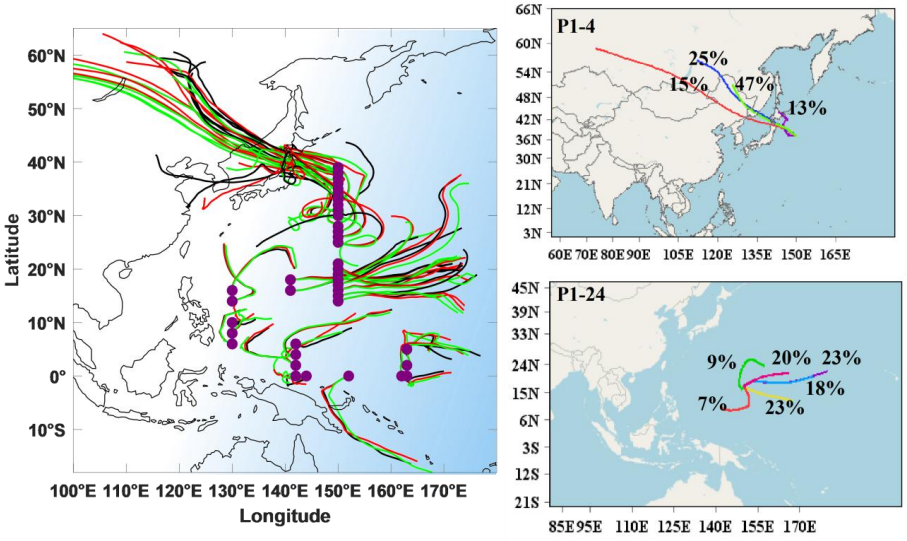

1135

1136 **Fig. 4.** Clusters of 96 h backward trajectories for different stations over the Western

1137 Pacific. The ensembled 96 h back-trajectories were within the lower troposphere

1138 above 10 m (red lines), above 100 m (black lines), and above 1000 m (green lines).

1139

https://doi.org/10.5194/egusphere-2025-251
Preprint. Discussion started: 24 February 2025

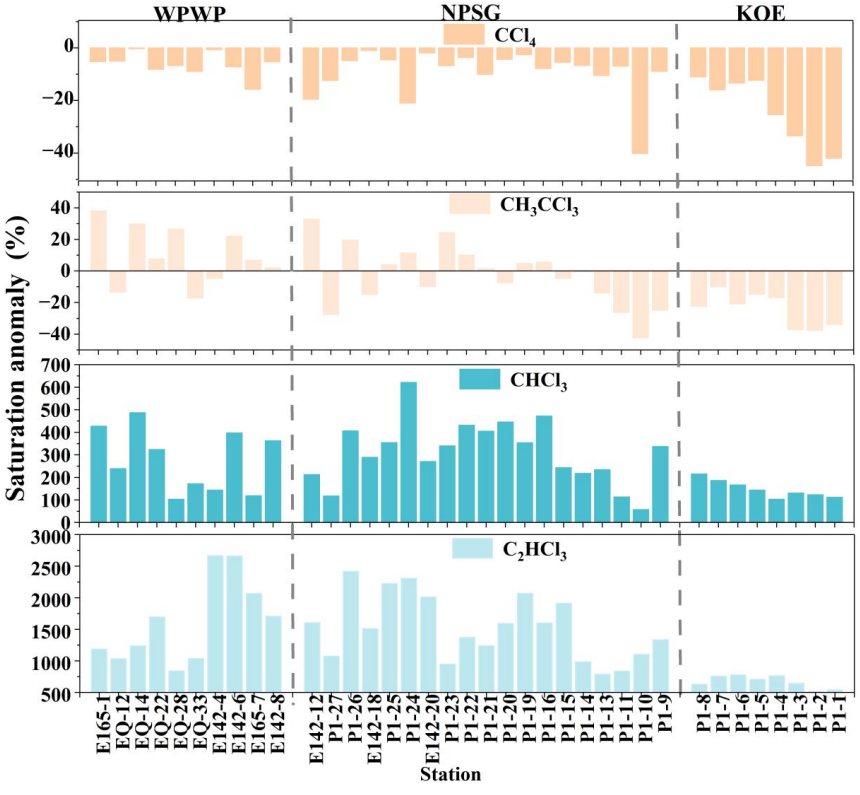

Fig. 5. Saturation anomaly of $CHCl_3$, CCl_4, C_2HCl_3, and CH_3CCl_3 in the Western Pacific.

https://doi.org/10.5194/egusphere-2025-251
Preprint. Discussion started: 24 February 2025

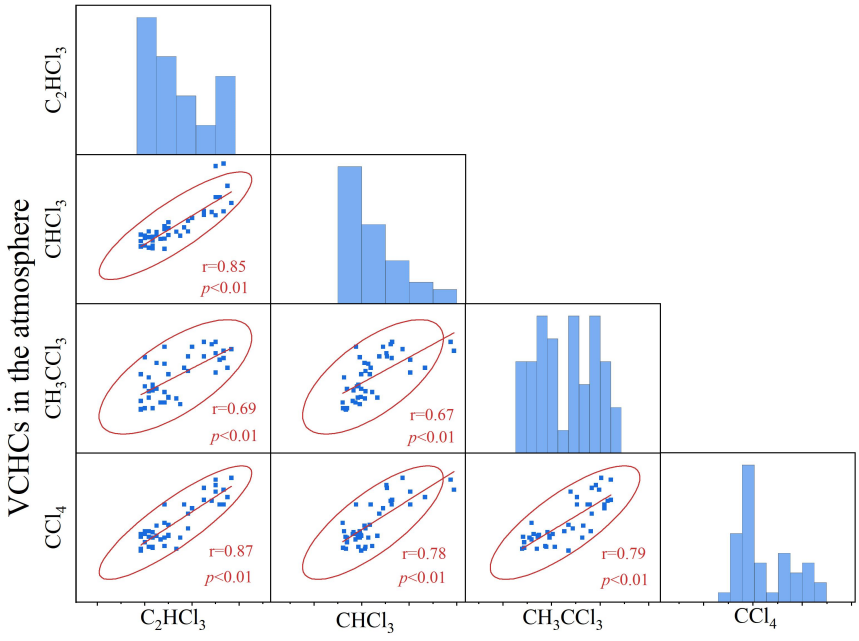

Fig. 6. Relationships between $CHCl_3$, CCl_4, C_2HCl_3, and CH_3CCl_3 in the atmosphere of the Western Pacific.

https://doi.org/10.5194/egusphere-2025-251
Preprint. Discussion started: 24 February 2025

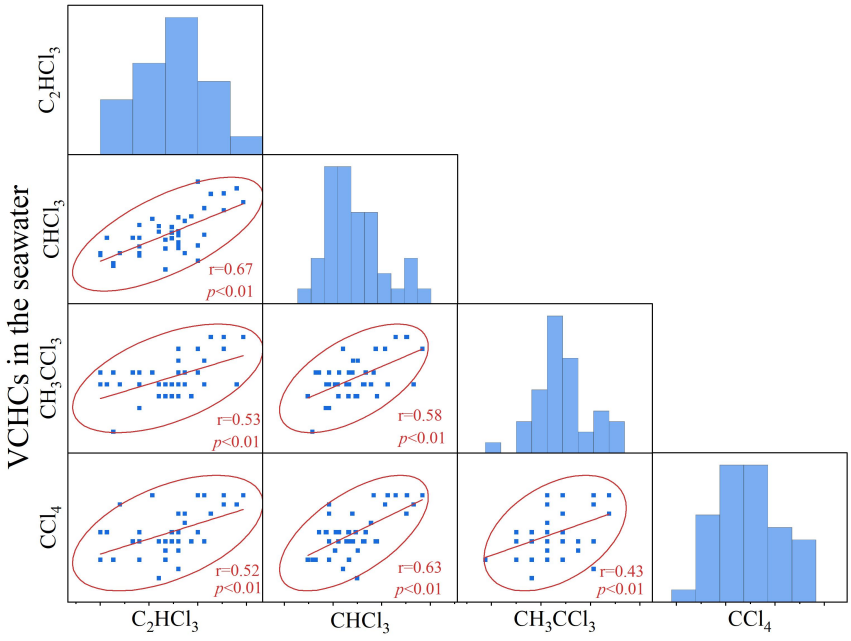

Fig. 7. Relationships between $CHCl_3$, CCl_4, C_2HCl_3, and CH_3CCl_3 in the seawater of the Western Pacific.

https://doi.org/10.5194/egusphere-2025-251
Preprint. Discussion started: 24 February 2025

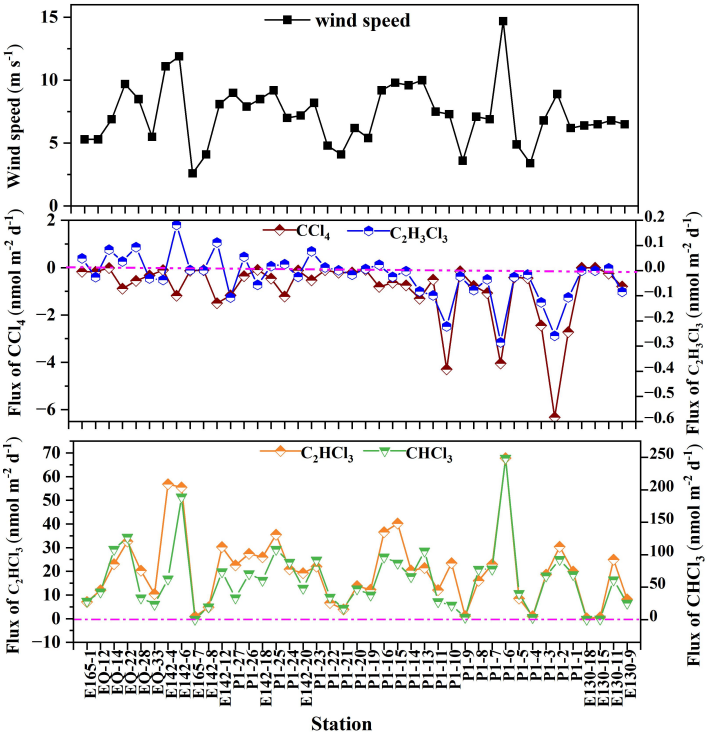

Fig. 8. Sea-air fluxes of $CHCl_3$, CCl_4, C_2HCl_3, and CH_3CCl_3, along with wind speeds in the Western Pacific.

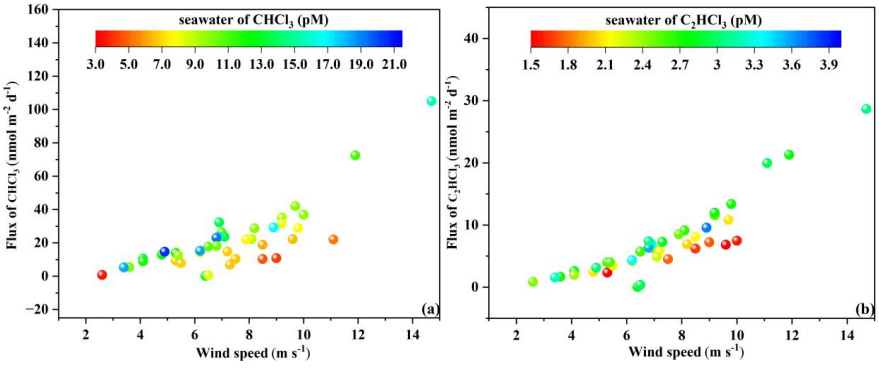

Fig. 9. Relationships between the sea-air fluxes of $CHCl_3$ (a) and C_2HCl_3 (b) and wind speed and seawater concentrations of $CHCl_3$ and C_2HCl_3 (points are colored according to seawater concentrations).

https://doi.org/10.5194/egusphere-2025-251
Preprint. Discussion started: 24 February 2025

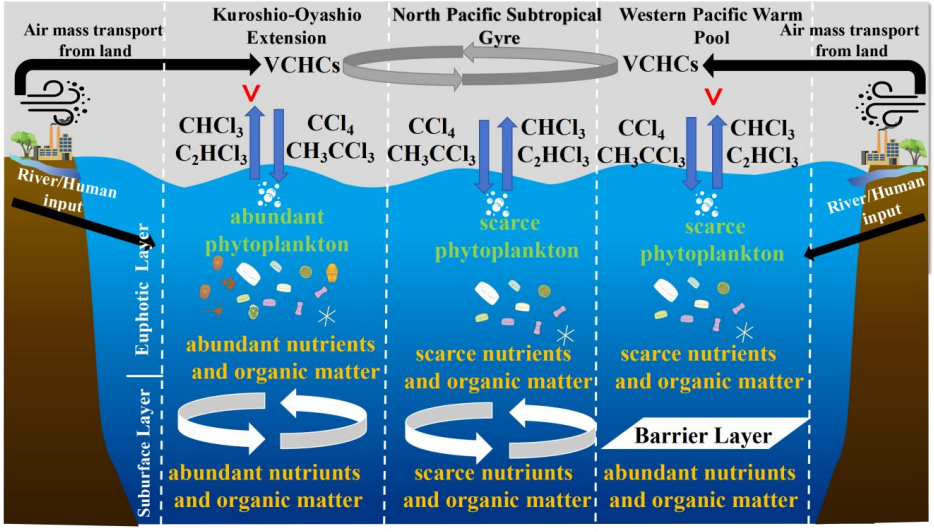

Fig. 10. Schematic diagram of key processes and factors controlling the production and distributions, as well as the sea-air interactions, of VCHCs in the Western Pacific.